Department of Physics and Astronomy

Heidelberg University

Master thesis

in Physics

submitted by

Moritz Epple

born in Berlin

2021

Two-Particle Quantum Interference and Bell's Theorem

This Master thesis has been carried out by Moritz Epple

at the

Max Planck Institute for Nuclear Physics

under the supervision of

Prof. Dr. Thomas Pfeifer

Two-Particle Quantum Interference and Bell's Theorem:

Bell's theorem is among the most challenging consequences of quantum mechanics. In this thesis, the connection between Bell's theorem and quantum interference is investigated by asking the question, whether Bell's theorem can be proven on the basis of two-particle quantum interference. In the first part of this thesis the meaning of quantum interference and Bell's Theorem for the discussion about the interpretation of quantum mechanics is retraced. By considering three major branches of interpretations, the conceptual difficulties, which are encountered in the face of quantum interference and Bell's theorem, are discussed. In addition, an epistemological argument for the inherent indeterminism of certain quantum mechanical phenomena is presented. In the second part of this thesis a two-particle quantum interference thought experiment is developed and it is shown that Bell's theorem can be proven from two-particle quantum interference, if certain quantum mechanical phenomena in the experiment are inherently indeterministic.

Zwei-Teilchen-Quanteninterferenz und Bells Theorem:

Bells Theorem ist eine der herausforderndsten Konsequenzen der Quantenmechanik. In dieser Arbeit wird die Verbindung zwischen Bells Theorem und Quanteninterferenz untersucht, indem der Frage nachgegangen wird, ob Bells Theorem auf der Grundlage von Zwei-Teilchen-Quanteninterferenz bewiesen werden kann. Im ersten Teil dieser Arbeit wird die Bedeutung von Quanteninterferenz und Bell's Theorem für die Diskussion über die Interpretation der Quantenmechanik nachvollzogen. Indem drei Hauptströmungen von Interpretationen betrachtet werden, werden die konzeptionellen Schwierigkeiten, die sich angesichts von Quanteninterferenz und Bells Theorem ergeben, besprochen. Außerdem wird ein epistemologisches Argument für die inhärente Indeterminiertheit von bestimmten quantenmechanischen Phänomenen präsentiert. Im zweiten Teil dieser Arbeit wird ein Zwei-Teilchen-Quanteninterferenz Gedankenexperiment entwickelt und es wird gezeigt, dass unter der Bedingung, dass bestimmte quantenmechanische Phänomene in dem betrachteten Experiment von Natur aus indeterministisch sind, Bells Theorem auf der Grundlage von Zwei-Teilchen-Quanteninterferenz beweisbar ist.

Acknowledgements:

It was the love, lively interest and support of my familiy, friends and teachers, which made this thesis possible. At foremost I want to thank my supervisor Prof. Thomas Pfeifer. I could not have imagined a better supervisor. The discussions with him were always inspiring and helped me to keep on track, when I was (once more) enthusiastically heading towards one of the dark abysses of physics. Also for his very helpful feedback on the manuscript and his commitment in general I want to thank him. I also want to thank Dr. Marco Masi, who supported this thesis a lot and whose remarks and comments on the manuscript were of great value for the clarity of this thesis. I am also especially thankful for the continuous support of my parents Bettina and Hans-Jörg with whom I lived together for the time of writing this thesis.

Contents

1 Introduction

The superposition principle and entanglement are at the heart of the disparity between classical physics and quantum mechanics. The one-particle superposition principle gives rise to interference phenomena and wave-particle duality, while entanglement, which might be seen as the superposition principle applied to systems with more than one variable, implies apparent *spooky actions at a distance* and leads to the rejection of local realism. A phenomenon that combines both features is two-particle interference. The most prominent example of two-particle interference is the double double-slit (DDS) experiment, which was introduced in 1993 by Greenberger, Horne and Zeilinger [1]. The experiment consists of two double-slit arrays and a particle source, which is placed midway between the two arrays and which emits momentum entangled particles. It proves to be the case that, while on the scintillation screens behind the individual double-slit arrays no interference patterns appear, a conditional interference pattern emerges, if the arrivals of the two particles are monitored in coincidence.

The DDS-experiment has been performed with photons [2] and electrons [3] and has also been considered for correlated Bose-Einstein condensates [4] and several other systems [5]. As mentioned in [4], the two particle interference pattern can be utilized to prove that the two particles are non-classically correlated. Since it is rather difficult to proof for massive particles that their correlations have a quantum origin [6], DDS-experiments with massive particles are especially relevant.

In this thesis, we examine the connection between two-particle interference and Bell's theorem [7]. More explicitly, we discuss a thought experiment, which is conceptually similar to the DDS experiment, and attempt to develop a proof of Bell's theorem for this specific setting along the lines of a proof given by Mermin [8].

In the part A of this thesis, we will introduce and develop the basic concepts, which we will further employ in the part B, where we discuss the thought experiment. The guiding theme for part A will be the interpretation of quantum mechanics. We have chosen to enter the subject from this rather conceptual point of departure, since it naturally connects the DDS-experiment with Bell's theorem as different aspects of the same struggle for a meaningful interpretation of the quantum formalism. Furthermore, this approach provides a natural context for introducing the necessary assumptions underlying Bell's theorem.

In the part B, we will then establish by means of an analogy a direct experimental

link between two-particle interference and Mermin's proof of Bell's theorem. It will be found that under the assumption that specific events are inherently indeterministic, Bell's Theorem can be proven from two-particle interference. At the end, we will summarize our results and give an outlook on future investigations.

Part A Overview:
Starting from the well-known double-slit experiment (section 2.1 and 2.2), we will trace our way through to more sophisticated quantum interference experiments, which will eventually lead us to the DDS-experiment (section 2.3). Then, after considering various possible interpretations of these experiments (section 2.4), we will focus on the explicit interpretation of the wave-function (section 2.5), which will guide us to Einstein, Podolsky and Rosen's argumentation in favor of hidden variables (section 2.6) and finally to Mermin's proof of Bell's theorem (section 2.7, 2.8, 2.9). We will conclude the part *A* with an argument for the existence of indeterministic events (section 2.10) and a summery (section 2.11).

Part B Overview:
After a description of the proposed experimental setting (section 3.1), we will develop the algorithm for the numerical determination of the time-evolved wave function for our experiment (section 3.2). The results of our calculation are presented thereafter: First we will make some general observations regarding the nature of two-particle interference in our experiment (section 3.3). Then, we will draw an analogy between our observations and the observations for a spin-$\frac{1}{2}$ particle in a Stern-Gerlach magnet (section 3.4), which will finally allow us to apply the scheme of Mermin's proof to our experiment (section 3.4). We will then discuss the validity of that scheme in the context of our experiment (section 3.5.3) and say a view words about possible experimental variations of the presented thought-experiment (section 3.6).

Appendix Overview:
In the Appendix we will introduce our notation for conditional probabilities (section 5.1), proof that it is impossible to detect any signs of determinism in certain quantum mechanical experiments (section 5.2), which is connected to our discussion about determinism in part *A* and derive the propagator for the free particle and the particle in a constant electric field, as well as some other results (section 5.3), which are needed for our calculation in part B.

2 Part A: Fundamental Concepts

2.1 Double-Slit Experiment

In the quantum mechanical double-slit experiment a particle source emits particles, one at a time, which propagate towards a detection screen. Between the particle source and the detection screen a barrier with two slits is placed (figure 1). While in the early days of quantum mechanics the double-slit experiment with single particles could only be considered as a thought experiment, nowadays it has been performed with electrons [9], neutrons [10], and also with atoms and massive molecules, such as the C_{60} fullerene [11].

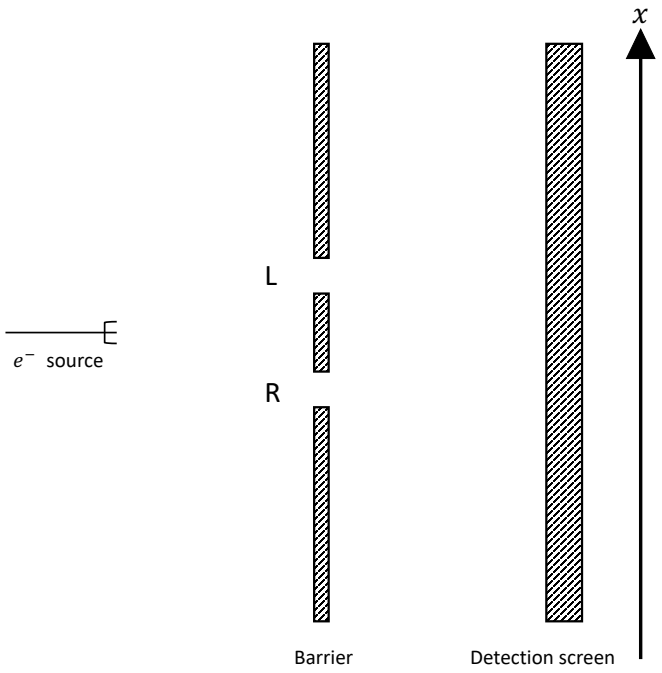

Figure 1: Schematic representation of the double-slit experiment for single electrons.

The measurement data of interest is the particle distribution on the detection screen after many emission cycles. We will call this distribution[1] $P(x)$. Before measuring $P(x)$ directly we could carry out the following experiment: First we close the *R-Slit* so that each particle, which is detected at the screen, has with certainty passed through

[1]In an actual experiment the detection screen would be divided into cells x_i and the distribution $P(x_i)$ would be obtained by counting the number of particles within each cell.

the *L-slit*. We then record the corresponding distribution $P_L(x)$. Then we close the *L-Slit* and record the distribution $P_R(x)$. One could naively expect that, if the particles pass equally likely through the R-slit as through the L-slit, $P(x)$ can be predicted from $P_L(x)$ and $P_R(x)$ by means of the equation

$$P_{cl}(x) = \frac{1}{2}(P_L(x) + P_R(x)). \tag{1}$$

The distributions $P_L(x)$ and $P_R(x)$ are similar to the distributions shown in figure 2a, which represents essentially what we would anticipate for some kind of solid, marble-like objects passing through a slit[2]. The distribution $P_{cl}(x)$ is depicted in figure 2b. However, 2b is not what is found if $P(x)$ is actually measured! The pattern that is found rather resembles the pattern shown in 2c.

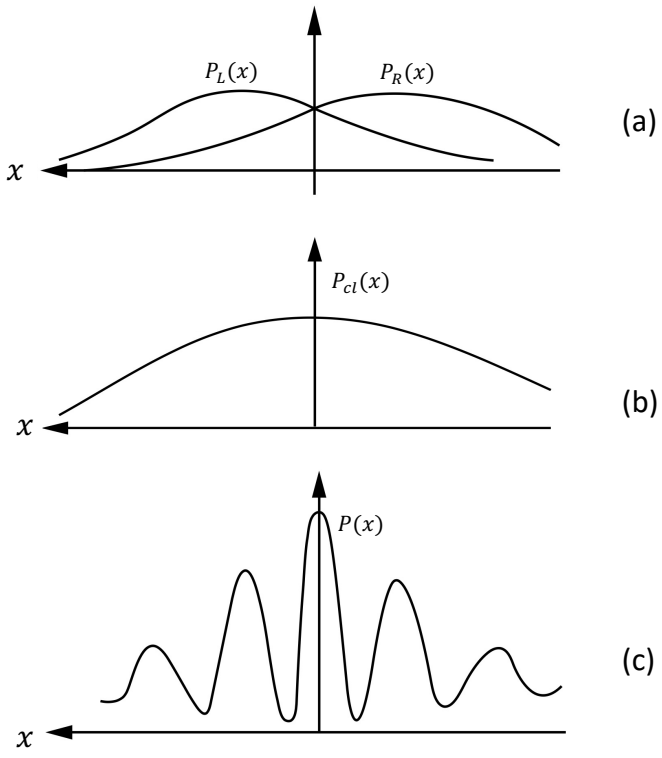

Figure 2: Double-slit distributions: (a) Distributions $P_L(x)$ and $P_R(x)$ for closed R-slit and closed L-slit respectively. (b) The sum-distribution: $P_{cl} = \frac{1}{2}(P_L(x) + P_R(x))$. (c) The actually measured interference distribution.

[2]If a greater portion of the screen would be shown and if the detection would be sensitive enough, one would actually detect single slit diffraction patterns. Although the distributions might look like gaussians, they really are the main lobes of something like sinc squared functions. Accordingly, a closer look reveals that the classical particle picture does not even work for the single slit detections (see e.g. [12]).

Even though nowadays the emergence of interference patterns in the double-slit experiment is a well established scientific fact, the phenomenon itself remains remarkable. Equation (43) surely is the way to go, if only one makes the classical assumption that each particle goes either through slit R *or* slit L. And according to our every-day experience, this is exactly what particles should do.

Thus the observed interference pattern, which reminds us of waves, emanating from two slits, interfering constructively and destructively, seems to suggest that something was wrong with our most reasonable *either-or* assumption, which led us to (43). To put it more frankly [13]: *We must conclude, that when both holes are open, it is not true that the particle goes through one hole or the other. For if it had to go through one or the other, we could classify all the arrivals at x into two disjoint classes, namely, those arriving through hole R and those arriving through hole L; and the frequency $P(x)$ of arrival at x would surely be the sum of the frequency $P_L(x)$ of particles coming through hole L and the frequency $P_R(x)$ of those coming through hole R.* So we are ready to conclude with Feynman that whenever both slits are open, the particle does *not* pass either through the R-slit *or* through the L-slit. But let us be cautious and ask whether Feynman's conclusion is inevitable?

A barrier with two open slits is different from a barrier with only one open slit and thus, even if the particles always pass through one slit or the other, the two-slit-barrier might interact differently with the particles than the one-slit-barrier and this difference might give rise to the different distributions 2b and 2c. Following this argumentation the frequency depicted in 2c could indeed be given by a sum of a frequency $\tilde{P}_L(x)$ of particles coming through the L-slit and a frequency $\tilde{P}_R(x)$ of particles coming through the R-slit, such that

$$P(x) = \frac{1}{2}(\tilde{P}_L(x) + \tilde{P}_R(x)), \tag{2}$$

only that now $\tilde{P}_L(x) \neq P_L(x)$ and $\tilde{P}_R(x) \neq P_R(x)$. An example of such a theory, which does actually reproduce all of the described measurement results, is Bohmian Mechanics [14, 15].

2.2 Quantum Formalism

In the quantum mechanical formalism the distribution $P(x)$ is determined from the wave function $\psi(x)$, which is a superposition of two components, one for each slit[3]. Assuming a symmetrical illumination of the slit, we can write

$$\psi(x) = \frac{1}{\sqrt{2}}(\varphi_L(x) + \varphi_R(x)), \tag{3}$$

where $\varphi_L(x)$ and $\varphi_R(x)$ are complex-valued functions of the independent variable x. According to Born's rule $P_L(x) = ||\varphi_L(x)||^2$ and $P_R(x) = ||\varphi_R(x)||^2$. Born's rule also tell us that $P(x)$ is given by

$$\begin{aligned} P(x) = ||\psi(x)||^2 = & \quad \frac{1}{2}\Big[||\varphi_L(x)||^2 + ||\varphi_R(x)||^2 + \varphi_L(x)\varphi_R^*(x) + \varphi_L^*(x)\varphi_R(x)\Big] \\ := & \quad \frac{1}{2}\Big[P_L(x) + P_R(x) + IT\Big]. \end{aligned} \tag{4}$$

The unexpected interference pattern of $P(x)$ thus results from the interference terms IT, as a direct consequence of the superposition of the two terms $\varphi_L(x)$ and $\varphi_R(x)$. One way to interpret this wave function formalism as a description of physical reality in the case of the double-slit experiment looks as follows: Each particle is prepared as a wave packet. This complex-valued wave packet itself is quite an unfamiliar object, but we will for now neglect such intricacies. While moving towards the barrier, the packet spreads out in space. At the barrier, one part of this wave moves through the R-slit and another part of it passes through the L-slit. The resulting two narrow wave packets also spread, while they keep on traveling towards the screen and thereby interfere with each other. Then, at some unpredictable time, this spread-out wave instantaneously collapses with the probability $P(x)$ to the single point, where the particle is finally found.

It is common practice to represent the wave function $\psi(x)$ as a state in abstract Hilbert-space:

$$|\psi\rangle = \frac{1}{\sqrt{2}}(|R\rangle + |L\rangle), \tag{5}$$

[3]In general we should consider a time dependent, three dimensional wave function $\psi(x, y, z, t)$. However, doing the calculation, it turns out that one can assume that

$$\psi(x, y, z, t) = \psi_x(x, t)\psi_y(y, t)\psi_z(z, t).$$

What we are actually considering then is $\psi_x(x, t)$ at the time of the detection of the particle at the detection screen. For more details about the full mathematical treatment of the double-slit experiment see [16].

where $|R\rangle$ represents $\varphi_R(x)$ and $|L\rangle$ represents $\varphi_L(x)$. Formally $|R\rangle$ and $|L\rangle$ form a basis of a two dimensional Hilbert space $\mathcal{H}$, which is connected to the the two-valued observable *which-slit*.

2.3 Which-Way Information

Our interpretation of the quantum formalism seems to tell us that the particles do not go either through the R-slit *or* the L-slit, but rather pass through the R-slit *and* the L-slit and that this behavior is the actual cause of the observed interference. However, as we have mentioned before, Bohmian Mechanics is capable of reproducing the interference pattern and in Bohmian Mechanics the particles obey the *either-or* assumption at all times. We thus ask ourselves: Do the particles *in reality* pass through either one slit *or* the other or do they pass through one slit *and* the other at the same time?

At the 1927 Solvay Congress in Brüssel, Einstein introduced a thought experiment [17], where *which-way-information*, i.e. knowledge about which slit the particles pass through, is determined from measuring the recoil of the double slit (see figure 3). The basic idea was that a particle which passes through R and reaches the point x_D suffers a different change in momentum Δp than a particle which passes through L and reaches x_D. But every change in the x-component of particle-momentum must be accompanied by an equal and opposite change in the momentum of the barrier. Therefore, measuring the momentum of the barrier before and after the passage of the particle is sufficient to know through which slit the particle has passed.

However, Bohr showed that according to Heisenberg's uncertainty principle $\Delta p \Delta x \leq \hbar/2$, if we know the momentum of the barrier *before* the passage of the particle with great accuracy, we have a correspondingly poor knowledge about the position of the barrier. This position uncertainty inevitably smears out the interference pattern. As it turns out, the position uncertainty is sufficient to wash out the interference pattern completely, such that only a distribution of the kind 2b remains [17, 13].

Somehow, just by detecting through which slit each particle passes, the distribution $P(x)$ of figure 2c, which reminded us of waves going through both slits at the same time, is replaced by the distribution $P_{cl}(x)$ of figure 2b, which is what we expected for marble-like tiny particles. Thus, even though we have found that every particle either takes one way *or* the other in Einstein's recoiling-slit experiment, we have lost the interference pattern along the way and it was the interference pattern, which we

wanted to understand in the first place.

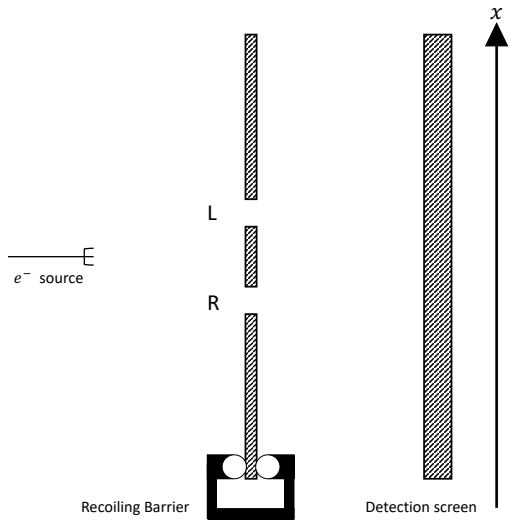

Figure 3: Einstein's recoiling slit experiment

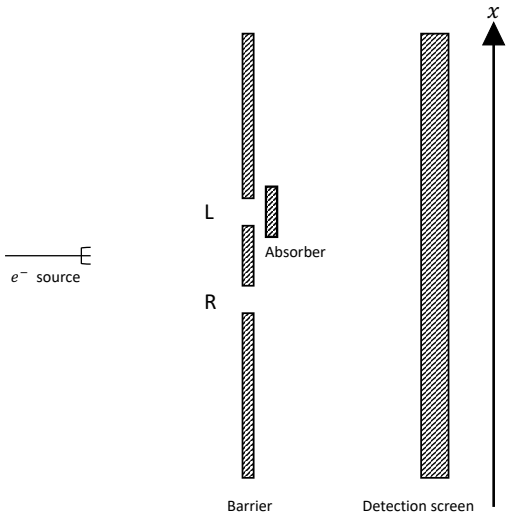

Figure 4: Double-slit experiment with absorber behind the L-slit

Within the quantum mechanical formalism the loss of interference can be explained by the introduction of *unpredictable* and *uncontrollable* phase factors α, β into the wave function of individual particles [18], such that it becomes

$$\psi'(x) = \frac{1}{\sqrt{2}}(\varphi_L(x)\exp(i\alpha) + \varphi_R(x)\exp(i\beta)). \tag{6}$$

In effect, the probability $P(x)$ for individual particles is transformed to

$$P'(x) = \frac{1}{2}\Big[||\varphi_L(x)||^2 + ||\varphi_R(x)||^2 + \varphi_L(x)\varphi_R^*(x)\exp(i[\alpha-\beta]) + \varphi_L^*(x)\varphi_R(x)\exp(i[\beta-\alpha])\Big], \tag{7}$$

where in comparison to (4) only the interference terms have been altered. Because the terms $\exp(i[\alpha-\beta])$ and $\exp(i[\beta-\alpha])$ will fluctuate in a random and uncontrollable way from run to run and because the interference pattern is only build up by many repetitions cycles, the interference terms will eventually average out to zero and no interference is observed.

In the time after Einstein's recoiling slit experiment many different experiments to gain which-way-information, have been considered and all of these experiments agree that as long as which-information-information is present, no interference appears. The quantum mechanical formalism accounts for all of the experimental results.

However, in 1971 Wootters and Zurek published an in depth analysis of Einstein's recoiling slit experiment in which they showed that it is possible to obtain partial which-way information and at the same time obtain an interference pattern with a reduced contrast [19]. The contrast of an interference pattern, also called *fringe-visibility* or just *visibility*, is defined by[4]:

$$\mathcal{V} = \frac{I_{max} - I_{min}}{I_{max} + I_{min}} \tag{8}$$

A simple way to obtain partial which-way-information in a double-slit experiment is to place an absorber behind one of the slits (see figure 4). If for example an absorber behind the L-slit absorbs the particles with a 99%-efficiency, we will know that 99% of all particles ending up at the detection screen have come through the R-slit. It turns out that in this case the visibility of the interference pattern is still about 20% of it's original visibility (with no absorber). One can show [20] that for this specific experiment the fringe-visibility and which-way-information fulfill the trade-off relation

$$\mathcal{V}^2 + \mathcal{P}^2 = 1, \tag{9}$$

where $\mathcal{P}$ is called *predictability* and is defined as $\mathcal{P} = |P(R) - P(L)|$ with $P(R)$ and $P(L)$ being the probabilities to pass through the R and the L-slit respectively. $\mathcal{P}$ is interpreted as an a priori knowledge about which path a particle will take. In the Hilbert-space representation (5) we can account for the absorber by introducing variable coefficients c_1 and c_2 such that

$$|\psi\rangle = c_1 |R\rangle + c_2 |L\rangle . \tag{10}$$

We can then express $\mathcal{P}$ and $\mathcal{V}$ by the coefficents c_1 and c_2 as $\mathcal{P} = |||c_2||^2 - ||c_1||^2|$ and $\mathcal{V} = |c_1 c_2^*|$. It follows that it is not true that interference fringes only occur under the condition that which-way-information is totally absent. Equation (9) tells us that there are intermediate cases, where partial which-way-information is compatible with an interference pattern of a reduced contrast.

Nevertheless, it is important to keep in mind that as long as $\mathcal{P} \neq 1$ we do *not* know, which way the particle takes. This means that we do not even know whether the particle takes one way *or* the other or whether it takes one way *and* the other at the same time. The term *which-way-information* and its interpretation as a priori knowledge can in this respect be quite misleading as it seems to suggest that there exists a specific way

[4]This definition applies especially to the case, where the contrast of the interference pattern is a constant, which is not true in general.

the particle takes and that we only have an incomplete knowledge about it. But this is exactly what seems to be defied by the cropping up of the interference pattern as soon as we don't know the way a particle takes with certainty (for related discussions see [21, 22]).
The double double-slit (DDS) experiment, which we have already mentioned in the introduction, is capable of demonstrating an even richer trade-off relation than the one depicted in (9).

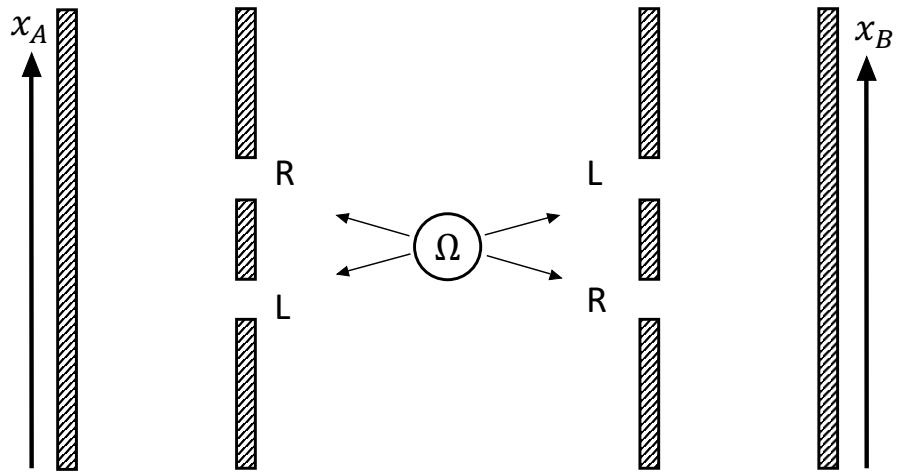

Figure 5: Schematic of the DDS experiment: A particle source Ω emits daughter particles, which individually pass through a double slit array.

In the DDS experiment we consider a mother particle Ω, which decays into two daughter particles A and B. A and B then move individually to a double slit ensemble as shown in figure 5. As discussed in [4], there are essentially two limiting cases:

- If Ω is tightly localized, there is no significant momentum correlation between the two particles: According to Heisenberg's uncertainty principle, the individual momentum wave packets have a large spread and measuring through which slit particle A has passed does not reveal through which slit B has passed and vice virsa. If neither for particle A nor for particle B a which-way-measurement is carried out, individual interference patterns emerge on the A and B-detection screen.

- If Ω is large, the individual momentum wave packets are small enough to imply a sufficiently high momentum correlation: If we carry out a which-way-measurement on the one particle, we also know through which slit the other

particle has passed. However, if we do not make a which-way-measurement and only detect A and B behind their respective double slits, we find a *conditional interference pattern* for A as well as for B. This means, we do not find an interference on the A or B-screen. But, if we consider only those A-runs, where B is detected at a specific spot x_{BD}, we find an A-interference pattern and similarly if we reverse the rolls.

If we further include the possibility of placing absorbers behind the A-slits and B-slits, we find the following trade-off relation for the DDS experiment [23]:

$$\mathcal{P}_i^2 + \mathcal{V}_i^2 + \mathcal{V}_{AB}^2 = 1, \tag{11}$$

where $i \in \{A, B\}$ and $\mathcal{V}_{AB}$ is the visibility of the conditional interference pattern described above. In terms of our Hilbert-space representation, the most general two-qubit state can be expressed as

$$|\Psi_{AB}\rangle = c_1 |R_A\rangle |R_B\rangle + c_2 |R_A\rangle |L_B\rangle + c_3 |L_A\rangle |R_B\rangle + c_4 |L_A\rangle |L_B\rangle . \tag{12}$$

As has been stated in [23] we can then express $\mathcal{P}_i$, $\mathcal{V}_i$, and $\mathcal{V}_{AB}$ in terms of the coefficients c_1, c_2, c_3, c_4:

$$\begin{aligned} \mathcal{P}_A &= |||c_3||^2 + ||c_4||^2 - ||c_1||^2 - ||c_2||^2|, \\ \mathcal{P}_B &= |||c_2||^2 + ||c_4||^2 - ||c_1||^2 - ||c_3||^2|, \end{aligned} \tag{13}$$

$$\begin{aligned} \mathcal{V}_A &= 2|c_1 c_3^* + c_2 c_4^*|, \\ \mathcal{V}_B &= 2|c_1 c_2^* + c_3 c_4^*|, \end{aligned} \tag{14}$$

$$\mathcal{V}_{AB} = 2|c_1 c_4 - c_2 c_3|. \tag{15}$$

The different experimental arrangements, which will either lead to perfect one particle predictability, perfect one particle interference, perfect conditional interference or any kind of intermediate phenomenon, can be modeled by the choice of the coefficients c_1, c_2, c_3, c_4. In the following, we will consider some special cases:

1. $\boxed{c_1 = c_2 = 0, c_3 = c_4 = \frac{1}{\sqrt{2}}}$

   The two-particle state is given by

$$|\Psi_{AB}\rangle = |L_A\rangle \frac{1}{\sqrt{2}}(|R_B\rangle + |L_B\rangle) \tag{16}$$

and $\mathcal{P}_A = \mathcal{V}_B = 1$, $\mathcal{V}_A = \mathcal{P}_B = \mathcal{V}_{AB} = 0$. This case corresponds to a measurement configuration, where no momentum correlation between A and B exists and where in addition we have placed a perfect absorber (100%) behind the R-slit of the A-barrier. We thus have a perfect single-particle interference pattern on the B-detection screen, but neither a single-particle interference pattern on the A-screen, nor a conditional interference pattern.

2. $\boxed{c_1 = c_2 = c_3 = c_4 = \frac{1}{\sqrt{2}}}$

   The two-particle state is given by

$$|\Psi_{AB}\rangle = \frac{1}{\sqrt{2}}(|R_A\rangle + |L_A\rangle)(|R_B\rangle + |L_B\rangle) \tag{17}$$

   and $\mathcal{V}_A = \mathcal{V}_B = 1$, $\mathcal{P}_A = \mathcal{P}_B = \mathcal{V}_{AB} = 0$. This is just the general case for a tightly localized source Ω, which leads to two single-particle interference patterns as described above.

3. $\boxed{c_1 = c_4 = \frac{1}{\sqrt{2}}, c_2 = c_3 = 0}$

   The two-particle state is given by

$$|\Psi_{AB}\rangle = \frac{1}{\sqrt{2}}(|R_A\rangle\,|R_B\rangle + |L_A\rangle\,|L_B\rangle) \tag{18}$$

   and $\mathcal{V}_A = \mathcal{V}_B = \mathcal{P}_A = \mathcal{P}_B = 0$, $\mathcal{V}_{AB} = 1$. This is the configuration, where the source Ω is large and the momenta of the particles are highly correlated. In contrast to the cases 1. and 2. all one particle quantities, i.e. $\mathcal{V}_A, \mathcal{V}_B, \mathcal{P}_A$ and $\mathcal{P}_B$ vanish and only a two particle quantity, namely $\mathcal{V}_{AB}$, is different from zero. We also notice that while in 1. and 2. the wave function $|\Psi_{AB}\rangle$ could be written as a *product state*, i.e. $|\Psi_{AB}\rangle = |\psi_A\rangle\,|\psi_B\rangle$, this is not possible anymore for the state of equation (18), which tells us that it is an *entangled state*. Interestingly, it turns out that $\mathcal{V}_{AB}$ as defined in (15) coincides with the concurrence $\mathcal{C}_{AB}$ for a pure two-qubit state [23], which has been identified by Wootters as an entanglement measure [24, 25]. A state with $\mathcal{V}_{AB} = \mathcal{C}_{AB} = 1$ is maximally entangled.

Besides the many experimental configurations, which we can capture in terms of certain values of the coefficients c_1, c_2, c_3, c_4 there are also experimental changes, which

are not captured in this way. As we have described above, in the case of a sufficiently large source Ω we still have the choice whether we want to gain which-way-information about the particles by measuring for A or B through which slit the particle goes, or we can decide to obtain a conditional interference pattern, if our arrangement is incapable of determining through which slit A and B pass.
Conceptually, all of these experiments tell us that there is a trade-off relation between several phenomena, which manifest itself under different experimental conditions. However, none of these experiments gives us a definite answer to our initial question. We can either determine through which slit the particles pass, but then we loose all interference phenomena or we can regain the interference at the expanse of loosing our ability to determine through which slit the particles pass, such that we can not exclude that they pass through both slits at the same time. It seems as if nature counts the answer to our initial question to one of her mysteries and she is not willing to reveal it at any price. With Bohr we could call to the phenomena, which manifest itself under different experimental configurations *complementary*, saying that they mutually exclude and complement each other[5].

2.4 Interpretations

The epistemological limitation, we have been describing at the end of the preceding paragraph, is a peculiar aspect of quantum mechanics. Bohr [17], Heisenberg [26] and Feynman [13] beautifully demonstrated the idea that Heisenberg's uncertainty relation in combination with the exchange of momentum and energy in the form of quanta with the energy $E = hf$ and momentum $\vec{p} = \hbar\vec{k}$, where f is the frequency and $\vec{k}$ the wave-number of the associated de-Broglie-wave, makes it impossible to gain new information about a quantum phenomenon (e.g. the interference pattern) without disturbing it substantially. These heuristic considerations, which do not make use of the full-fledged quantum formalism, still have an important lesson to teach. They illustrate that in the quantum experiment it is *in principle* impossible to know certain things: It is *in principle* impossible to *infer* which way the particle takes, when interference is observed. It is also *in principle* impossible to *predict* the position of a particle at a time $t_0 + \Delta t$, if at the time t_0 a position measurement is carried out (and if Δt is not infinitesimally small)[6]. This situation is fundamentally different from everything we

[5]We won't go into the details of Bohr's conception of complementary, which is quite complex. For a short but concise discussion see [21].

[6]which is just a restatement of Heisenberg's uncertainty principle

know in the context of classical physics. In classical physics we might also be unable to *infer* or to *predict* certain properties of a physical system, but there *in principle* it is always possible to rearrange our measurement apparata such that we are able to infer or predict the missing piece of information *without* disturbing the observed phenomena substantially.

An epistemological limitation per se does not mean that the world does not have a well-defined structure beyond that boundary of our knowledge. For Kant for example it was clear that we could know nothing about the *thing in itself*. But he nevertheless considered the question for the nature of the thing in itself as very meaningful. However, one might also take the position that the epistemological boundary of the world coincides in some sense with the ontological boundary of the world and that it is meaningless to speak of properties, which can *in principle* not be known. This is essentially the perspective Bohr and Heisenberg had on quantum mechanics. According to this interpretation, it is meaningless to ask whether the particle went through one slit *or* the other or whether it went through one slit *and* the other at the same time. Nature simply does not have an answer to that question. The appeal of that position in the context of quantum mechanics stems from delivering a kind of explanation for the unfamiliar epistemological limitations inherent to quantum mechanical observations. For if there exists no representable and analyzable *structure beyond* it becomes obvious that we are unable to find such a structure.

Including our previous remarks, we can essentially distinguish three different branches of possible interpretations of quantum mechanics[7]:

- **Formalistic Interpretations ($\mathbf{I_F}$)**: Interpretations, which interpret the quantum formalism as some kind of description of physical reality. This includes especially all interpretations, which consider the wave function as a description of the actual state of the physical system.
- **Hidden Variables Interpretations ($\mathbf{I_{HV}}$)**: Interpretations, which assume that there is a more detailed description of physical reality than given by the wavefunction, e.g. Bohmian Mechanics.
- **Epistemic Interpretations ($\mathbf{I_E}$)**: Interpretations, which state that it is meaningless to speak of properties, which can not be known in principle.

[7]With interpretation we mean theories, which lead to the same experimental predictions (as quantum mechanics), but differ on their meta-level and therefore in their conceptual understanding of the predictions. For a similar account see [27].

Note that **($\mathbf{I_E}$)** does not necessarily imply that the wave function is nothing more but a *representation of knowledge*. For David Bohm for example **($\mathbf{I_E}$)** implied that [28] *the wave function is an abstraction, providing a mathematical reflection of certain aspects of reality, but not a one-to-one mapping*, which is quite a different conception.

2.5 The Problem with the Wave Function

Since the wave function accounts for all possible predictions, **($\mathbf{I_F}$)** seem to be promising candidates for an appropriate interpretation of quantum phenomena. However, taking the wave function as a description of physical reality turns out to be problematic for several reasons. According to the standard formulation of quantum mechanics along the lines of von Neumann [29], there exist two dynamical laws for the time evolution of the wave function:

1. *Linear dynamics:*
   As long as no measurement is carried out, the state $|\psi\rangle$ evolves in a *linear* and *deterministic* way. That is $|\psi(t_1)\rangle = \mathbf{U}(t_1, t_0)\,|\psi(t_0)\rangle$, where $\mathbf{U}(t_1, t_0)$ is a unitary operator, given by:
   $$\mathbf{U}(t_1, t_0) = \exp\Big(-\frac{i}{\hbar}\mathbf{H}(t_1 - t_0)\Big) \tag{19}$$
   with $\mathbf{H}$ being the Hamilton-operator of the system.

2. *Nonlinear collapse dynamics:*
   If a measurement is carried out at the time t the wave function $|\psi(t)\rangle$ collapses with the probability $P(a_i) = ||\,\langle a_i|\psi(t)\rangle\,||^2$ *nonlinearly* and *instantaneously* to an eigenstate $|a_i\rangle$ of the observable $\mathbf{A}$ being measured.

The most straight forward reason, why these two dynamical laws are problematic is the *measurement problem*: According to the linear dynamics of the wave function, two physical systems, which interact with each other, become entangled. If one assumes, that measurement devices are physical systems[8] this is problematic. According to the first dynamical law, by interacting with the object under observation, a measurement-device should end up in an entangled state with the observed object, where neither the measuring device nor the object under investigation is in a well-defined state. But this directly contradicts the prediction of the second dynamical law. Thus, as long as no

[8]Given that we normally think of measurement devices as conglomerates of physical systems, namely electrons, protons and neutrons, this is a reasonable assumption.

criterion is given, which tells us why measurement-devices are distinct from ordinary physical systems, standard quantum mechanics leads to contradictory predictions.
It was this contradiction, which led Everett to the formulation of his theory of the universal wave-function [30]. Everett's strategy to avoid the measurement problem is essentially to keep the wave-function as a description of physical reality, but to drop the collapse dynamic. However, Everett's theory and it's successors have their own problems with explaining why we have determinate experiences in a wavefunction-universe [31]. The same holds true for all considerations, which try to explain the classical appearance of the macroscopic world by invoking *decoherence*. Decoherence simply does not solve the measurement problem [32].
Note however that the problem arises in the first place from *interpreting* the wave function as a description of physical reality. If we rather consider the wave function as a tool to calculate the probabilities for well-defined observable phenomena, the problem disappears; no collapse is needed then.
There is also another problem with the collapse dynamic: It is not Lorentz-covariant. When an electron is found on the detection screen, its wave function *instantaneously* goes to zero everywhere except at the point where it is found. However, in special relativity different observers have different standards of simultaneity, such that what is simultaneous in one frame of reference is not simultaneous in another frame and thus a wave-function, which instantaneously goes to zero everywhere, but at a single point, can not exist in special relativity [33, 34]. Again, the problem lies not in the quantum mechanical probabilities, but rather in the interpretation of the wave function as physically real. We will return to this issue later.
These considerations make clear that it is desirable to find alternatives to $\mathbf{(I_F)}$. One way to try to find a way out of these affairs, is to hypothesize that real particles are characterized by properties, which have specific values at all times and that the indefiniteness of the wave function, the collapse postulate and all of the follow-up problems are just artifacts of an incomplete formalism. This strategy, which matches the $\mathbf{(I_{HV})}$ type of interpretation, is basically what Einstein, Podolski and Rosen (EPR) had in mind when they presented their argumentation in favor of hidden variables.

2.6 EPR

In their seminal paper [35] EPR argue that quantum mechanics does not provide a complete description of physical reality. More concretely, EPR show that according

to a specific *reality criterion* the wave function does not provide complete information about the values of all in reality existing physical quantities of a physical system. EPR's reality criterion **(RC)** reads:

(RC): *If, without in any way disturbing a system, we can predict with certainty (i.e. with probability equal to unity) the value of a physical quantity, then there exists an element of reality corresponding to that quantity.*

If we carry out a measurement on a physical system, which is prepared in the state $|a_i\rangle$, where $|a_i\rangle$ shall be an eigenstate to some observable $\mathbf{A}$, we find with certainty (probability equal to unity) the eigenvalue a_i. However, if an observable $\mathbf{B}$, which does not commute with $\mathbf{A}$ ($[\mathbf{A}, \mathbf{B}] \neq 0$) would be measured, no definite prediction for the outcome of the measurement could be made. According to **(RC)**, while the physical quantity $\mathbf{A}$ has to be considered an element of physical reality, the physical quantity $\mathbf{B}$ can not be predicted with certainty from the wave function and therefore fails to meet the criterion, *if* the wave function is a complete description of reality. EPR thus conclude: *From this follows, that either*

1. *the quantum mechanical description of reality given by the wave function is not complete or*
2. *when the operators corresponding to two physical quantities do not commute the two quantities cannot have simultaneous reality.*

EPR's paper is about showing that 1. is true. Their strategy to achieve this is to prove that 2. must be wrong and therefore 1., being the only alternative, must be true. To show this EPR consider a system composed of two particles A and B. They assume that after a time t_0 there is no interaction between A and B and at a time t_1 ($t_1 > t_0$) the two particles are described by the entangled wave function

$$\psi(x_A, x_B, t_1) = \int_{-\infty}^{\infty} dp \exp\left(\frac{i}{\hbar} p(x_A - x_B)\right) = 2\pi\hbar \int_{-\infty}^{\infty} dx \delta(x_B - x)\delta(x - x_A), \quad (20)$$

where we have expanded the wave-function in two different bases, namely the basis of momentum eigenstates and the basis of position eigenstates. From this wave function two pieces of information can be obtained.

- If at t_1 particle A is found to have the momentum p, a momentum measurement on particle B at t_1 gives with *certainty* the result $-p$ and vice virsa.

- If at t_1 particle A is found at the position x, a position measurement on particle B at t_1 will with *certainty* find the particle at $-x$.

According to **(RC)** the position of B at t_1 is an element of reality, if the position of A is measured at t_1 and the momentum of B at t_1 is an element of reality, if the momentum of A is measured at t_1. But since there is no interaction between A and B, whether momentum or position is measured on particle A can have no influence on particle B and therefore, EPR conclude, both properties must be elements of reality, which contradicts 2. and therefore proves 1.
There are a few comments in place about EPR's argumentation. First note that if one rejects **(RC)** the whole argumentation becomes invalidated. In the same year that EPR published their paper Bohr wrote a response defending $\mathbf{(I_E)}$ against EPR's argumentation [36]. Bohr's main point was that any experimental arrangement suited to measure one of the two non-commuting observables p and x, makes it impossible to have any knowledge about the value of the other observable, which for Bohr meant that any statement about the other observable is meaningless. Thus for Bohr **(RC)** failed to be a sufficient reality criterion, which allowed him to reject EPR's line of reasoning.

Besides **(RC)** the probably most important assumption in EPR's argumentation is that no interaction takes place between A and B after the time t_0. How can we know that two particles are not interacting with each other? Even if we would be able to exclude any kind of mechanical or electromagnetic coupling between A and B, how could we exclude that the particles are not interacting by means of some unknown kind of force or field? Surely, in general we can not exclude such interactions. However, as long as we adhere to SR we can argue that events, which are space-like separated, can not exert any influence on each other.
Consider for example the spacetime-diagram in figure 6. If the A-measurement is carried out at t_1 and the B-measurement at t_3 a signal, traveling with the speed of light, could inform particle B about the A-measurement outcome, such that it could behave correspondingly. But if, for example, the B-measurement is carried out at t_2 no subluminal or luminal signal could transmit such information. Thus, by choosing a proper spacetime-configuration one can exclude (given that SR is valid) any information exchange between the two particles, which is sufficient to justify EPR's no interaction assumption.
Being more precise, the spacetime-configuration should not only exclude the possibility that information about a *measurement outcome* is transmitted to the other particle before it is detected, it should also exclude the possibility that information about the

measurement configuration is transmitted. Thus, even if we only set the A-measurer at t_1, we want to detect particle B at t_2 or earlier, such that no information about the choice of measurement configuration can be transmitted.

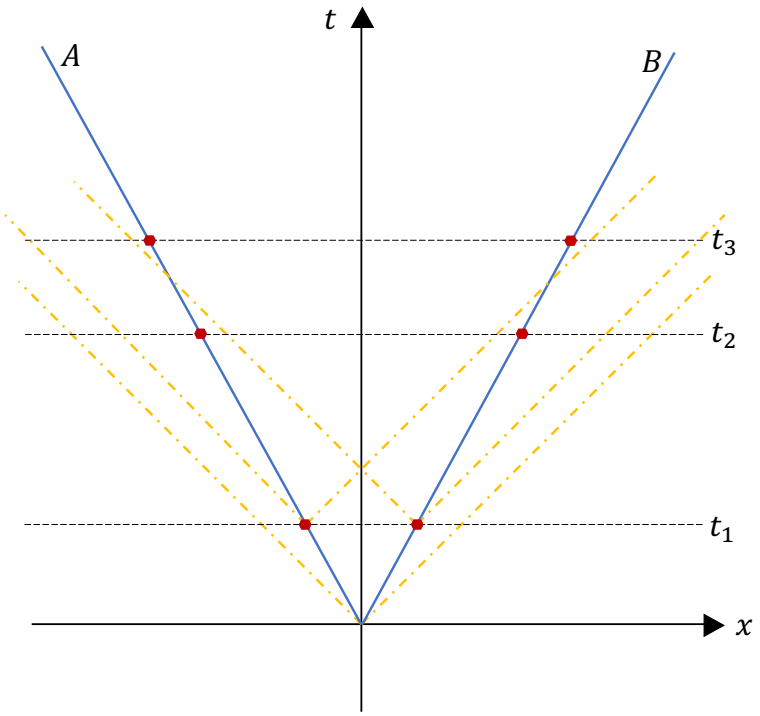

Figure 6: Spacetime-diagram of possible measurement scenarios: The blue lines represent the world lines of the particles. The dashed yellow lines symbolize the world lines of light-signals and the red dots mark possible measurement events.

2.7 Hidden Variables and Bell's Theorem

If one accepts **(RC)** and EPR's no interaction assumption, their argumentation is valid and there should exist a more fine-grained formalism than standard quantum mechanics. Technically, all hidden variable (HV) interpretations $\mathbf{(I_{HV})}$ share the following characteristics [37]:

- The elements of physical reality are represented by hidden variables λ.
- The ensemble of identical systems is in the same macrostate, but the individual systems on the ensemble might be in different microstates, labelled by different values λ.

- The outcome of a measurement on an individual system is determined by the values of λ, directly in the so-called deterministic HV theories, or by means of a probability distribution in the stochastic HV theories.

Note that according to this characterization standard quantum mechanics as discussed in section 2.5 is a stochastic HV theory. Let us call for now all HV theories, which do not conflict with SR, *local HV theories*. In 1964 Bell proved that local HV theories are not compatible with quantum mechanics [7]. This result is known as *Bell's Theorem*. Bell proved it, by deriving an inequality (*Bell's inequality*), which must be fulfilled by all local HV theories, which however is violated by quantum mechanics. In a series of experiments during the early 80s Alain Aspect and coworkers gave the first experimental verification of Bell's theorem [38, 39, 40], demonstrating that nature fully agrees with the quantum mechanical predictions. By refining the experiments in 2015 three groups separately achieved a "loop-hole free" experimental verification of Bell's Theorem [41, 42, 43]. In the following section we will consider Mermin's proof of Bell's theorem [8], which will also be essential for the B-part of this thesis.

2.8 Mermin's Proof of Bell's Theorem

2.8.1 The Setting

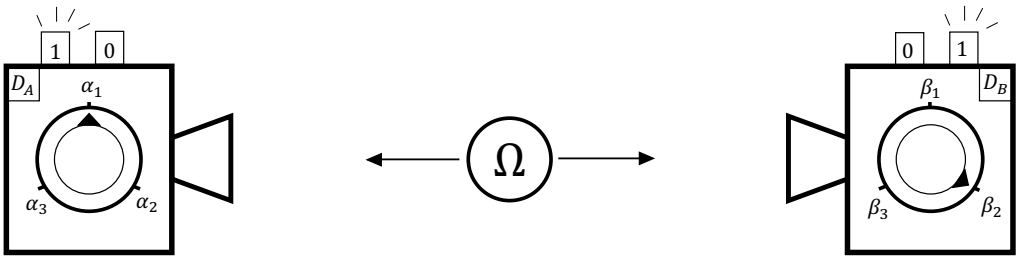

Figure 7: Experimental set-up for Mermin's proof of Bell's theorem: A source Ω emits two spin $\frac{1}{2}$-particles A, B in the singlet-state, which fly to detectors D_A, D_B, where the particles are measured in one of three possible measurement-configurations $\alpha_1, \alpha_2, \alpha_3$ ($\beta_1, \beta_2, \beta_3$), which are chosen freely by the experimentalists. If spin-up is found the zero-light flashes, if spin-down is found the one-light flashes.

Mermin considers a particle source Ω, which produces two spin $\frac{1}{2}$-particles (A, B) in the singlet state:

$$|\Psi_{AB}\rangle = \frac{1}{\sqrt{2}}(|0_A\rangle\,|1_B\rangle - |1_A\rangle\,|0_B\rangle), \tag{21}$$

where we have identified *spin-up* along some perpendicular axis to the propagation direction with 0 and *spin-down* along the same axis with 1. As depicted in figure 7 the particles fly apart to two different detectors D_A and D_B . The experimentalists can choose between three different measurement settings, which are denoted by $\alpha_1, \alpha_2, \alpha_3$ ($\beta_1, \beta_2, \beta_3$). Each measurement configuration corresponds to a specific orientation of a Stern-Gerlach magnet. By turning the Stern-Gerlach magnet about $2\pi/3$ in the plane perpendicular to the axis of propagation one can switch from one setting to another. For each measurement-configuration A and B will either be found to have spin-up or spin-down. If spin-up is found, the detector flashes the zero-light, if spin-down is found, the detector flashes the one-light. We will assume with Mermin that the detector settings are chosen completely random, such that $p(\alpha_i) = p(\beta_i) = 1/3$ for all i.
If we would carry out many runs of this experiment and noted down for every run the configuration of D_A and D_B, as well as which light has flashed, quantum mechanics tells us that the data should exhibit the following two features:

- If the settings of D_A and D_B are the same, i.e. if $i = j$ for α_i and β_j, the results of the two measurers always *disagree*, i.e. whenever D_A flashes the 0-light, D_B flashes the 1-light and whenever D_A flashes the 1-light, D_B flashes the 0-light.
- If one considers an *arbitrary* run of the experiment, the probability $P(+)$ that D_A and D_B flash the *same* light is given by $P(+) = \frac{1}{2}$.

As we will see, local HV theories can not be rendered compatible with these two features.

2.8.2 The Quantum Mechanical Point of View

Let us start by deriving the quantum mechanical prediction. We can represent the states of a spin-$\frac{1}{2}$ particle by points on the *Bloch-sphere* (figure 8). Let us choose to place the spin-up state along the z-axis $|0\rangle$ at the north pole and the spin-down state along the z-axis $|1\rangle$ at the south pole. Then, any other state can be represented by

$$|\theta, \varphi\rangle = \cos\left(\frac{\theta}{2}\right)|0\rangle + \exp(i\varphi)\sin\left(\frac{\theta}{2}\right)|1\rangle\,, \tag{22}$$

which allows a unique identification of states and points on the sphere.

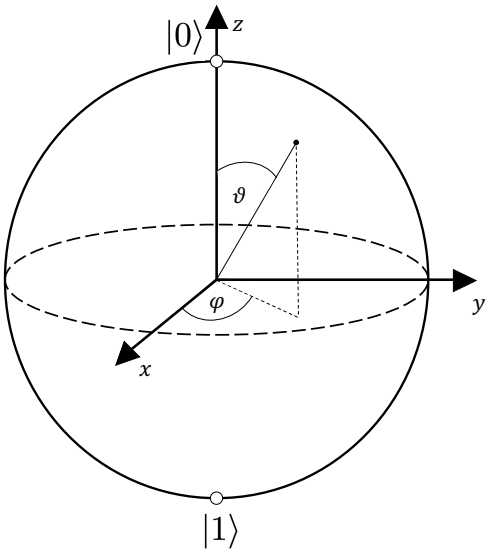

Figure 8: Bloch-sphere: Each qubit state can be represented as a point on the Bloch-sphere.

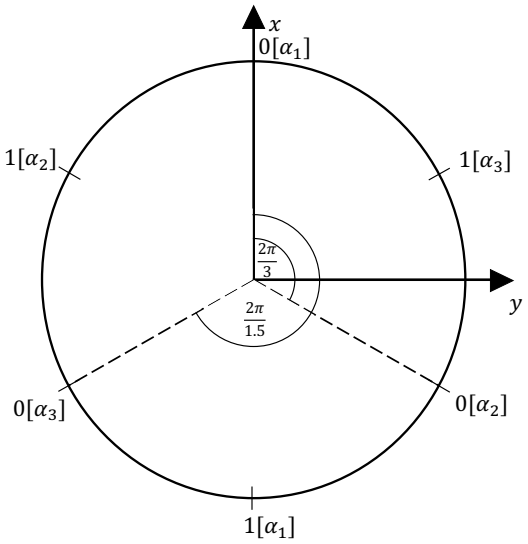

Figure 9: Relevant points on the Bloch-sphere for Mermin's proof of Bell's theorem. All of the points are separated from their neighbor points by $\frac{2\pi}{6}$.

Preparing a spin-$\frac{1}{2}$ particle in the state $|\theta, \varphi\rangle$ and measuring the spin along the z-axis yields spin-up with probability

$$P(0) = \cos^2(\theta/2) = \frac{1}{2}(1 + \cos(\theta)) \tag{23}$$

and spin-down with probability

$$P(1) = \sin^2(\theta/2) = \frac{1}{2}(1 - \cos(\theta)). \tag{24}$$

For any state which lies on the equator it holds that $P(0) = P(1) = \frac{1}{2}$. Rather than expressing all states in terms of $|0\rangle$ and $|1\rangle$, one could choose any other two opposite points on the sphere, which would represent the spin-up $|\uparrow\rangle$ and the spin-down $|\downarrow\rangle$ along the axis connecting both points. We could then define angles θ' and φ' in order to express all states by an expression similar to (22).
As one can verify by direct calculation, two spin-$\frac{1}{2}$ particles (A, B), which are initialized in a singlet-state according to one basis (e.g. $\{|0\rangle, |1\rangle\}$), also form a singlet state according to any other basis (e.g. $\{|\uparrow\rangle, |\downarrow\rangle\}$), such that

$$|\Psi_{AB}\rangle = \frac{1}{\sqrt{2}}(|0_A\rangle\,|1_B\rangle - |1_A\rangle\,|0_B\rangle) = \frac{1}{\sqrt{2}}(|\uparrow_A\rangle\,|\downarrow_B\rangle - |\downarrow_A\rangle\,|\uparrow_B\rangle). \tag{25}$$

We know that in the quantum mechanical formalism the probability $P(a_j, b_k)$ to obtain in a joint measurement the A-result a_j and the B-result b_k is given by:

$$P(a_j, b_k) = || \langle a_j, b_k | \Psi_{AB} \rangle ||^2. \tag{26}$$

The conditional probability $P(a_j|b_k)$ to obtain a_j given b_k is defined by[9]:

$$P(a_j|b_k) = \frac{P(a_j, b_k)}{P(b_k)}, \qquad P(b_k) = \sum_{j=1}^{N} P(a_j, b_k). \tag{27}$$

Applying these laws to the singlet state directly reproduces the first feature of our data, i.e. the perfect anti-correlation for measurements along the same axis (for the notation see figure 9):

$$\begin{aligned} P\big(0[\alpha_i]\big|0[\beta_i]\big) = P\big(1[\alpha_i]\big|1[\beta_i]\big) = P\big(0[\beta_i]\big|0[\alpha_i]\big) = P\big(1[\beta_i]\big|1[\alpha_i]\big) = 0, \\ P\big(0[\alpha_i]\big|1[\beta_i]\big) = P\big(1[\alpha_i]\big|0[\beta_i]\big) = P\big(0[\beta_i]\big|1[\alpha_i]\big) = P\big(1[\beta_i]\big|0[\alpha_i]\big) = 1. \end{aligned} \tag{28}$$

In order to derive the second feature of the data, note that we can define the probability $P(+)$ that D_A and D_B flash the same light by

$$P(+) = P(0_A, 0_B) + P(1_A, 1_B) = P(0_A|0_B)P(0_B) + P(1_A|1_B)P(1_B). \tag{29}$$

We can then define the *conditional state* $|\Psi_{Ak}\rangle$ of particle A given that B is found in the state $|b_k\rangle$ by the equation

$$|\Psi_{Ak}\rangle := \frac{\langle b_k|\Psi_{AB}\rangle}{\sqrt{P(b_k)}}. \tag{30}$$

If for example the B-spin is found to be in the state spin-up up along the axis β_2 ($0[\beta_2]$), according to (30) the conditional A-spin state is spin-down along α_2. As can be seen in figure 9, the point on the Bloch-sphere, which represents the spin-down along α_2 ($1[\alpha_2]$) lies $\frac{2\pi}{6}$ away from the spin-up state along α_1 ($0[\alpha_1]$) and the spin-up state along α_3 ($0[\alpha_3]$). Thus, from our discussion above, we know that the conditional probability $P(0[\alpha_1]|0[\beta_2])$ to find spin-up for A along α_1 under the condition that for B we have found spin-up along β_2 is given by

$$P\big(0[\alpha_1]\big|0[\beta_2]\big) = \frac{1}{2}(1 + \cos\Big(\frac{2\pi}{6}\Big)) = \frac{3}{4} \tag{31}$$

[9]See Appendix 5.1 for the definition of conditional probabilities

and similarly for $P(0[\alpha_3]|0[\beta_2])$. Thus, if we take into account that all α_i measurement configurations are equally likely, we obtain

$$\begin{aligned} P\big(0_A\big|0[\beta_2]\big) &= \frac{1}{3}\Big\{P\big(0[\alpha_1]\big|0[\beta_2]\big) + P\big(0[\alpha_2]\big|0[\beta_2]\big) + P\big(0[\alpha_3]\big|0[\beta_2]\big)\Big\} \\ &= \frac{1}{3}(\frac{3}{4} + 0 + \frac{3}{4}) = \frac{1}{2}. \end{aligned} \tag{32}$$

But, due to the symmetry of the experiment, we obtain the same result, if we exchange β_2 with β_1 or β_3. We can thus conclude that $P(0_A|0_B) = 1/2$. Carrying out the same calculation for $P(1_A|1_B)$, we also find that $P(1_A|1_B) = 1/2$. Thus from equation (29) we can conclude that

$$P(+) = P(0_A|0_B)P(0_B) + P(1_A|1_B)P(1_B) = \frac{1}{2}(P(0_B) + P(1_B)) = \frac{1}{2}, \tag{33}$$

which reproduces the second feature of the data.

2.8.3 The Hidden Variables Point of View

The first feature of our data tells us that we know with certainty (probability equal to unity) the spin-value of the A particle given the spin-value of the B-particle and vice virsa, if we measure the A-spin and B-spin along the same axis. Thus, given an appropriate spacetime-configuration, **(RC)** tells us that the spin-values for all three measurement configurations are elements of reality. These elements of physical reality should then be represented by hidden variables λ.

Let us see how we come to the same conclusion even without taking **(RC)** for granted. Using the notation of figure (9) we know, for example, that the conditional probability that D_A flashes the 0-light in the configuration α_i (particle A has spin-up along the axis α_i) under the condition that the hidden variables are given by λ and that D_B also flashes the 0-light in the configuration β_i (particle B also has spin-up along the same axis β_i) is given by:

$$P\big(0[\alpha_i]\big|\lambda, 0[\beta_i]\big) = 0. \tag{34}$$

However, since we are only considering *local* hidden variables, nothing which happens with particle B can have any influence on the A-measurement (given an appropriate spacetime-configuration) and thus it must hold that

$$P\big(0[\alpha_i]\big|\lambda, 0[\beta_i]\big) = P\big(0[\alpha_i]\big|\lambda\big) = 0 \qquad \Longleftrightarrow \qquad P\big(1[\alpha_i]\big|\lambda\big) = 1. \tag{35}$$

But equation (35) tells us that the value of the A-spin along the axis α_i is completely determined by the hidden variables λ, which is just another way of saying that the spin-value must be encoded in the hidden variables. It doesn't matter for our argumentation in what kind of physical incarnation this information is encoded and we will simply say that the particles carry *instruction sets*, which determine the spin-values. We might for example write a certain instruction set for particle A as 110 saying that for α_1 the answer is 1, for α_2 1 and for α_3 0. This A-instruction set implies the B-instruction 001. For if A and B are measured along the same axis, they must be anti-correlated. The instruction sets can be classified into two classes:

- Class 1:
  All instructions with two equal numbers: $101, 110, 011, 001, 010, 100$.
- Class 2:
  All instructions with three equal numbers: $111, 000$.

Let us now consider the probability $P(+)$ that D_A and D_B flash the same light. It turns out that $P(+)$ has the same value for all instructions in the same class, so it will suffice to consider two exemplary cases.
Let us start with the instruction $(001_A, 110_B)$. For each of the nine possible joint measurement configurations we have a certain outcome, which is determined by the given instruction:

Configuration (D_A, D_B)	$\alpha_1\beta_1$	$\alpha_1\beta_2$	$\alpha_1\beta_3$	$\alpha_2\beta_1$	$\alpha_2\beta_2$	$\alpha_2\beta_3$	$\alpha_3\beta_1$	$\alpha_3\beta_2$	$\alpha_3\beta_3$
Flashing lights (D_A, D_B)	01	01	00	01	01	00	11	11	10

These are *four* cases in which A and B flash the same light and *five* cases in which they flash different lights. The *nine* measurement configurations of D_A and D_B are chosen completely random. Thus we determine that $P(+) = \frac{4}{9}$. This result holds true for all other instructions from the class 1. For the class 2 we consider $(000_A, 111_B)$. As can be directly seen $P(+) = 0$. This implies

$$\boxed{P(+) < \tfrac{4}{9}} \tag{36}$$

for *all* local HV theories. The *Bell inequality* (36) is violated by quantum mechanics, which (as we have seen above) predicts that $P(+) = \frac{1}{2} > \frac{4}{9}$. Note that the violation of

the inequality (36) depends strongly on the angles between the different measurement configurations. If we would have chosen e.g. three right angled orientations of the Stern-Gerlach magnets, we would not have found any violation.

2.9 Assumptions Underlying Bell's Theorem

Our derivation of Bell's inequality crucially relied on a cluster of three assumptions, which we will now discuss in some more detail. These assumptions are *statistical independence*, *parameter independence* and *outcome independence*:

- **Parameter Independence**:
  Parameter independence states that for a given microstate λ the probability for a D_A-outcome a_n is independent from the experimental setting β_j of the device D_B:

  $$P(a_n|\beta_j, \lambda) = P(a_n|\beta_k, \lambda) = P(a_n|\lambda). \tag{37}$$

  We have already mentioned this condition verbally in our discussion about EPR's no interaction assumption in section 2.6. We said that, as long as SR is not violated, this assumption can be assured by a proper spacetime-configuration of the experiment. Given such a proper spacetime-configuration, equation (37) leads to the following *no-superluminal-signalling* condition[10]:

  $$P(a_n) = \int d\lambda \sum_m P(a_n, b_m|\beta_j, \lambda)P(\lambda) = \int d\lambda \sum_m P(a_n, b_m|\beta_k, \lambda)P(\lambda). \tag{38}$$

  If (38) were not true, one could send superluminal messages just by changing the B-measurement configuration. However, note that (37) is a stronger condition than (38), i.e. (37) can be violated, while at the same time (38) is not. Bohmian Mechanics, for example, violates (37), but does not violate (38). This is due to the fact that in Bohmian Mechanics it matters whether the B-measurement or the A-measurement is carried out first [44]. The dynamic of the particles depends on this order, which contradicts (37) *and* special relativity. However, as it is impossible to know the exact state of the particles to a better degree than

[10] One derives (38) from (37) by the use of the equation:

$$\sum_m P(a_n, b_m|\beta_j, \lambda) = P(a_n|\beta_j, \lambda)$$

the wave function allows, still no superluminal signaling is possible in Bohm's theory [45].

- **Outcome Independence**:
  Outcome independence states that the measurement-outcomes at D_A are independent from the outcomes at D_B:

$$P(a_n|b_m, \lambda) = P(a_i|b_l, \lambda) = P(a_n|\lambda). \tag{39}$$

  We have also discussed this assumptions in section 2.6. We came to the conclusion that special relativity assures the validity of (39) for proper spacetime-configurations. Note that if we treat the wave function as a description of physical reality, quantum mechanics violates (39): The probability to find a_i under the condition that particle B is measured to have the property b_j and that λ is given by $|\Psi_{AB}\rangle$ depends crucially on b_j. The violation of (39) is directly connected to the clinch between the collapse postulate and SR, which we discussed in section 2.5.

Parameter independence and outcome independence taken together are often referred to as *factorability* or *Bell locality-condition* [37]. Mathematically, we can express the factorability condition by combining (37) and (39):

$$P(a_i|b_j, \beta_k, \lambda) = P(a_i|\lambda). \tag{40}$$

Equation (40) is the general expression of (35), which we applied in the previous section 2.8.3. However, even if (35) is fulfilled, there is still a way to surpass our conclusion that local HV theories must specify three-valued instructions sets in the context of the presented experiment. The remaining loophole is a violation of statistical independence.

- **Statistical Independence**:
  Statistical independence states the the hidden variables λ are independent from the detector settings. We may express this condition mathematically as:

$$P(\lambda|\alpha_i, \beta_j) = P(\lambda) \tag{41}$$

By means of Bayes' Theorem[11] we can rewrite this assumption as:

$$P(\alpha_i, \beta_j|\lambda) = P(\alpha_i, \beta_j) \tag{42}$$

Let us focus on two special cases, which represent possible violations of (41) and (42). One way to read equation (41) would be to understand it as expressing that hidden variables ($\lambda(t)$) can not be influenced by a *posterior* choice (at $t' > t$) of the measurement-configuration. On this interpretation a violation of (41) would mean the existence of *retrocausality*. *Retrocausality* does not directly violate SR, as the *direction* of causality does not follow from the light-cone-structure. However, retrocausality leads to various paradoxes, which would have to be resolved by additional assumptions. Another way to understand statistical independence, which is more explicitly expressed in (42), is that it assures that the measurement-configurations are chosen *freely*. More concretely, this means that the choice of measurement configuration does not depend on the hidden variables λ. Note that in contrast to parameter and outcome independence, which are based on an experimentally tested physical theory (SR), statistical independence is a *plausability* assumption. The reason why statistical independence is assumed is simply that most physicists deem it unlikely that the measurement configuration depends on λ. Theories, which violate statistical independence are often referred to as *superdeterministic* theories. For a recent discussion in favor of superdeterminism see [46].

2.10 Determinism

In the terminology of above it can be said that a HV theory is deterministic, if the conditional probability $P(a_i|\ \alpha_m, \lambda)$ is either equal to 0 or 1 for all possible measurement outcomes a_i [47]. Since physics is an empirical science one can ask under what circumstances observational data suggest an underlying deterministic structure.
Given a repeatable experiment it might be said that determinism is suggested whenever two pieces of data a_i and b_j appear to fulfill the relationship[12] $P(a_i|b_j)$ is equal to 0 or 1. On the other hand, if for an event a_i no event b_j is found, such that $P(a_i|b_j)$ is equal to 0 or 1, this might suggest that the event a_i has no deterministic origin.
The measurement results in quantum mechanical experiments come in both types. The

[11] See Appendix 5.1.
[12] The observational data in classical mechanical experiments are exactly of that type.

singlet-state, which we considered in section (2.8) gave rise to perfectly anti-correlated measurement results, which (as we have seen in equation (28)) fulfill the property "$P(a_i|b_j)$ equal to 0 or 1". On the other hand, we noticed in section (2.8.2) that pure single electron states, which are initialized in the spin-up state along the z-axis ($|\psi(t_0)\rangle = |0_z\rangle$) and measured along the x or y-axis, give spin-up 0_x, 0_y with probability $P(0_x) = P(0_y) = 1/2$, such that e.g. no correlation of the form "$P(0_x|b_j)$ equal to 0 or 1" is found.
However, quantum mechanics even goes beyond that by saying that it is *in principle* impossible to prepare an experiment with the outcome probabilities $P(0_x) = P(0_y) = 1/2$, $P(0_z) = 1$ (as in the case of $|\psi(t_0)\rangle = |0_z\rangle$) and to observe in the same experiment an event b_j such that "$P(0_x|b_j)$ equal to 0 or 1" is fulfilled. As is shown in Appendix 5.2, this is a consequence of the trade-off relation (11), which for the present case can be rewritten as

$$(2P_A(0_x) - 1)^2 + (2P_A(0_y) - 1)^2 + (2P_A(0_z) - 1)^2 + \mathcal{C}_{AB}^2 = 1, \tag{43}$$

where $\mathcal{C}_{AB}$ is the concurrence, which was introduced in our discussion of the DDS-experiment in section 2.3. This means that in a world, where (43) holds, it is impossible to find any sign of determinism for certain quantum mechanical events[13], which, from an empirical point of view, strongly suggests that these events inherently indeterministic.

To make our point more clear, let us consider the above spin-$\frac{1}{2}$ particle experiment with outcome probabilities $P(0_x) = P(0_y) = 1/2$, $P(0_z) = 1$ in a HV theory setting. For deterministic HV theories it holds that $P(0_x|\ \alpha_x, \lambda)$ is either equal to 0 or 1. It follows from our above considerations that in a world, where (43) holds, this implies that deterministic HV theories are either wrong or can not be distinguished experimentally from (partially) indeterministic HV theories for which $P(0_x|\ \alpha_x, \lambda)$ is not equal to 0 or 1. The crucial point here is the mentioned observation that the trade-off relation (43) entails that the two statements:

1. $P(0_x|\ \alpha_m, \lambda)$ is either equal to 0 or 1.

2. $P(0_x) = P(0_y) = \frac{1}{2}$, $P(0_z) = 1$.

are incompatible, *if* λ *is experimentally available*. From this follows that either λ can be determined experimentally, which would imply that $P(0_x|\ \alpha_x, \lambda)$ can not be equal

[13]For example, the event 0_x in an experiment, which is characterized by outcome probabilities $P(0_x) = P(0_y) = 1/2$, $P(0_z) = 1$.

to 0 or 1 and thus prove deterministic HV theories to be wrong, or λ can not be determined experimentally, which would make deterministic HVs theories empirically indistinguishable from (partially) indeterministic ones as defined above. This is just another way of saying that in a world, where (43) holds, it is impossible to find any signs of determinism for the event 0_x and it was argued above that in such a world it would be reasonable to assume (at least from an empirical point of view) that the event 0_x is indeed inherently indeterministic. In general, for inherently indeterministic events a_i, it would hold that there exist no elements of reality, which could be represented by hidden variables λ, such that λ determines whether a_i is found or not, i.e. such that $P(a_i|\alpha_i, \lambda)$ is equal to zero or one.
While the trade-off relation (43) for electrons has to our knowledge not been examined experimentally, several related trade-off relations have been verified experimentally [48, 49, 50] and there is no reason to believe that the quantum mechanical prediction (43) would be violated. Accordingly, the given argumentation would suggest that the event 0_x in the considered experiment is an inherently indeterministic event. If the argumentation for the spin-$\frac{1}{2}$ particle example can be generalized to arbitrary quantum systems, it would furthermore be suggested that all measurement outcomes a_i, for which according to quantum mechanics in a given experiment no event b_j is found such that $P(a_i|b_j)$ is equal to 0 or 1, are inherently indeterministic events.

2.11 Summary Part A

In figure 10 we have summarized the content of this chapter graphically. We started by considering the double-slit experiment and one-particle quantum interference, which seemed to be at odds with the idea of particles traveling on a single well-defined path, even though we could not exclude that possibility completely. With the aid of the wave function $\psi(x)$ and Born's rule we were able to predict the characteristic statistical behavior of the particles.
By considering more sophisticated experiments, such as Einstein's recoiling-slit experiment and the DDS experiment, we were confronted with certain trade-off relations, which told us that there is a certain complementarity between several phenomena, which manifest itself under different experimental conditions. They also raised our awareness of the fact that there ist an epistemological limitation in quantum mechanics completely foreign to classical physics, which makes it impossible to answer certain questions, such as whether the particle goes through one slit *or* the other or whether

it goes through one slit *and* the other in the presence of interference.
By interpreting this epistemological limitation as a manifestion of the absence of an analyzable and describable *world beyond*, we were led to a branch of interpretations of quantum mechanics, which holds that it is meaningless to speak of properties, which can not be known *in principle*. We referred to this branch with **($\mathbf{I_E}$)**. Since the quantum mechanical formalism and in particular the wave function $\psi(x)$ is capable of predicting the statistical behavior of quantum particles, we introduced another branch of interpretations **($\mathbf{I_F}$)**, which incorporated all those interpretations, which took the wave function as a representation of physical reality.
By going into the details of **($\mathbf{I_F}$)** we were faced with the measurement-problem and the failure of Lorentz-covariance. We tried to overcome the problem by assuming, in conformity with our third branch of interpretation **($\mathbf{I_{HV}}$)**, that the problem arises in the first place as an artifact of an incomplete formalism. However, while non-local HV theories as Bohmian Mechanics have their own problem with Lorentz-covariance, Bell's theorem tells us that local HV theories are not compatible with the predictions of quantum mechanics. It follows that as long as the predictions of special relativity and quantum mechanics are considered to be valid, it seems like neither **($\mathbf{I_F}$)** nor **($\mathbf{I_{HV}}$)** can lead to a satisfactory explanation of quantum phenomena.
In principle many worlds interpretations might be able to save **($\mathbf{I_F}$)**, however, until now no satisfactory many worlds interpretation has been found [31]. On the side of **($\mathbf{I_{HV}}$)**, superdeterministic theories have the potential to incorporate the predictions of SR and QM into a meaningful interpretation. But our argumentation in section 2.10 shows that (super)deterministic theories are not only unsupported by present-day empirical evidence, but also by all *possible* empirical evidence, as long as the relevant quantum mechanical predictions agree with experiment.
Another way to walk the fine line between quantum non-locality and SR is **($\mathbf{I_E}$)**. By refraining from the question *when* the values of the spins become definite, **($\mathbf{I_E}$)** evades to make any statements, which could contradict SR. Accordingly, **($\mathbf{I_E}$)** essentially amounts to saying that it is meaningless to speak of a particular time, when the values of the spins become definite. However, most physicists would probably assume that in reality the values of the spins become definite at a certain time (if they accept in accordance with Bell's theorem that they were not definite all the time). But if one assumes that in reality the values of the spins become definite at a certain time, the contradiction with SR is there and it does not really matter whether we can know that time or not.

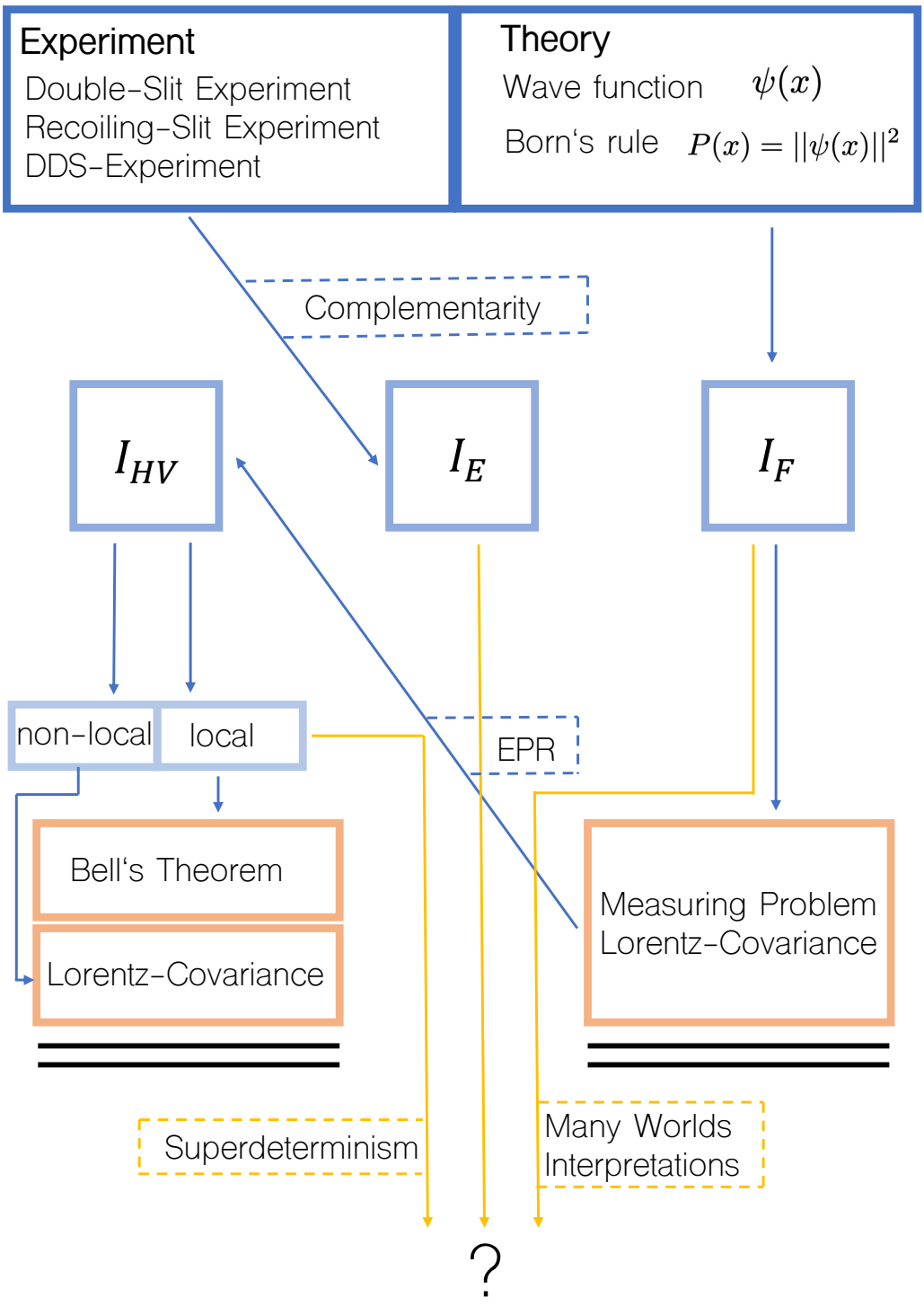

Figure 10: Representation of the part A content: Detailed description of the figure is given in the text above.

3 Part B: Results

3.1 Two-Particle Interference Thought Experiment

We consider the dissociative photoionization of an atom (or molecule) by means of a two-color laser. According to [51] a two-color laser can be created with the help of an optical arrangement as depicted in figure 11. A fundamental beam with a central frequency ω_2 passes through a beamsplitter. Half of the beam is directed to a non-linear optical medium, such as a BBO-crystal[14], where by means of *harmonic generation* n photons with the frequency of the central beam create a photon with the frequency $\omega_1 = n \cdot \omega_2$. The remaining laser-light with the frequency ω_2 is then filtered out with a dichroic mirror and the beam with photons of the frequency ω_1 is combined with the other half of the fundamental beam of frequency ω_2.

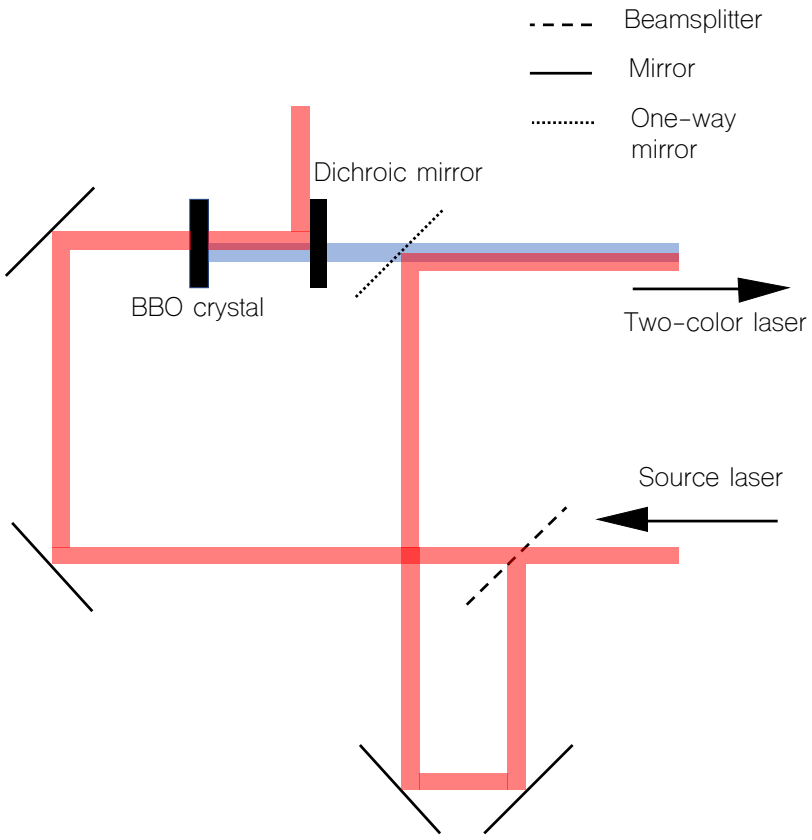

Figure 11: Schematic representation of a Mach-Zehnder interferometer for the production of two-color laser light.

[14]For high harmonic generation other techniques would have to be applied, see e.g. [52, 53]

The two-color laser is then directed towards the atom, which is assumed to be at rest with respect to the laboratory system. In effect the atom can undergo a number of possible dissociative ionization channels. For our purpose, we want to consider a dissociation, which leads to two charged, distinguishable fragments A and B.
Note that we can not distinguish a priori between the two ionization-alternatives (ionization by high or by low energetic photons). Only by carrying out measurements on the fragments of the ionization in a suitable basis[15], we can know whether the atom has been ionized by a photon with energy $E_1 = \hbar\omega_1$ or by a photon with energy $E_2 = \hbar\omega_2$. Consequently, before the measurement the two alternatives interfere and the wave function of the ionization-fragments A and B is a superposition of two components, one for each energy.
If we only consider the motion of the fragments perpendicular to the laser propagation axis, due to momentum conservation A and B fly in opposite directions with approximately equal momenta. Assuming a gaussian profile for the individual A and B wave packets and reducing our analysis to one dimension, which is chosen to be the propagation direction of the two fragments in the plain perpendicular to the laser propagation axis, we can model the entangled AB-wave function at a time t_0 shortly after dissociation by:

$$\Psi_{AB}(x_A, x_B, t_0) = \frac{1}{\sqrt{2}}\Big\{\varphi_1(x_A, t_0)\tilde{\varphi}_1(x_B, t_0) + \varphi_2(x_A, t_0)\tilde{\varphi}_2(x_B, t_0)\Big\} \tag{44}$$

with

$$\begin{aligned}
\varphi_j(x_A, t_0) &= (2\pi\sigma_0^2)^{-1/4} \exp\Big(- \frac{(x_A - x_{A0j})^2}{4\sigma_0^2}\Big) \exp\Big(ik_{0j}(x_A - x_{A0j})\Big), \\
\tilde{\varphi}_j(x_B, t_0) &= (2\pi\sigma_0^2)^{-1/4} \exp\Big(- \frac{(x_B - x_{B0j})^2}{4\sigma_0^2}\Big) \exp\Big(- ik_{0j}(x_B - x_{B0j})\Big),
\end{aligned} \tag{45}$$

where the different energies E_1 and E_2 (with $E_1 > E_2$) are encoded in k_{01} and k_{02}, which are connected to the momenta of the particles by $p_{01} = \hbar k_{01}$ and $p_{02} = \hbar k_{02}$ (such that $p_{01} > p_{02}$). The wave function (45) can thus be understood as a superposition of two components $\varphi_1(x_A, t_0)\tilde{\varphi}_1(x_B, t_0)$ and $\varphi_2(x_A, t_0)\tilde{\varphi}_2(x_B, t_0)$, whereas the first component $\varphi_1(x_A, t_0)\tilde{\varphi}_1(x_B, t_0)$ represents two wave packets, which travel in opposite directions with a "high" momentum p_{01}, while the second component $\varphi_2(x_A, t_0)\tilde{\varphi}_2(x_B, t_0)$ repre-

[15] If E_1 and E_2 are chosen appropriately, a simple position measurement of the fragments at a later time t could distinguish between E_1 and E_2. This follows from the proportionality of energy and momentum and the fact that if t is chosen large enough position measurements at t can be seen as momentum measurements at t_0 [54].

sents two wave packets, which travel in opposite directions with a "low" momentum p_{02}.

From the high and low momentum wave packets $\varphi_1(x_A, t_0)$ and $\varphi_2(x_A, t_0)$ associated with particle A and the high and low momentum wave packets $\tilde{\varphi}_1(x_B, t_0)$ and $\tilde{\varphi}_2(x_B, t_0)$ associated with particle B, we can calculate the distributions $||\varphi_j(x_A, t_0)||^2$, $||\tilde{\varphi}_j(x_B, t_0)||^2$, which are normal distributions with x_{A0j} and x_{B0j} as mean values and σ_0 as standard deviation (see figure 13a). If E_1 and E_2 are chosen appropriately, the corresponding momentum distribution[16] $P(p_A, p_B, t_0) = ||\Psi_{AB}(p_A, p_B, t_0)||^2$ implies a perfect AB-correlation for the two-valued momentum observables O_A and O_B, which can either have the value *high* (H) or *low* (L) as explained in the caption of figure 12.

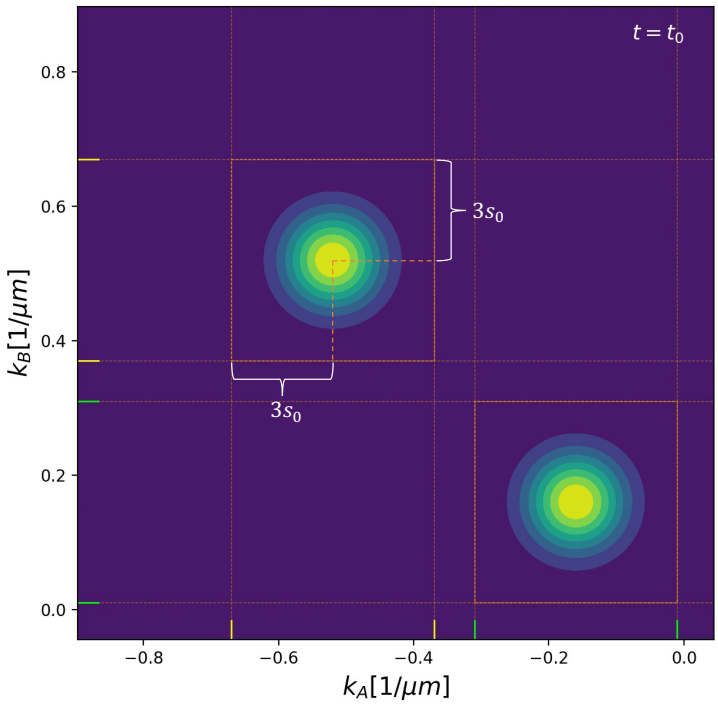

Figure 12: Density plot of momentum distribution $P(p_A, p_B, t_0) = ||\Psi_{AB}(p_A, p_B, t_0)||^2$: If we define momentum observables O_A, O_B, which either have the value *high* (H), when the momentum is found in between the two yellow bars or *low* (L), when the momentum is found in between the two green bars, O_A and O_B are perfectly correlated, i.e. $O_A = H \Leftrightarrow O_B = H$ and $O_A = L \Leftrightarrow O_B = L$. The parameters, which were used for the plot, are the same as the parameters given at the beginning of section 3.3. The standard deviation s_0 for the initial momentum distributions $||\varphi_j(p_A, t_0)||^2$, $||\tilde{\varphi}_j(p_B, t_0)||^2$ is given by: $s_0 = \frac{1}{2\sigma_0}$.

[16] $\Psi_{AB}(p_A, p_B, t_0)$ is obtained from $\Psi_{AB}(x_A, x_B, t_0)$ by the application of a two-dimensional Fourier-transform.

If k_{01} and k_{02} are positive, the mean values of $||\varphi_j(x_A,t)||^2$ travel in the negative x-direction for increasing t, while the mean values of $||\tilde{\varphi}_j(x_B,t)||^2$ travel in the positive x-direction. Simultaneously the width of all distributions increases with t.

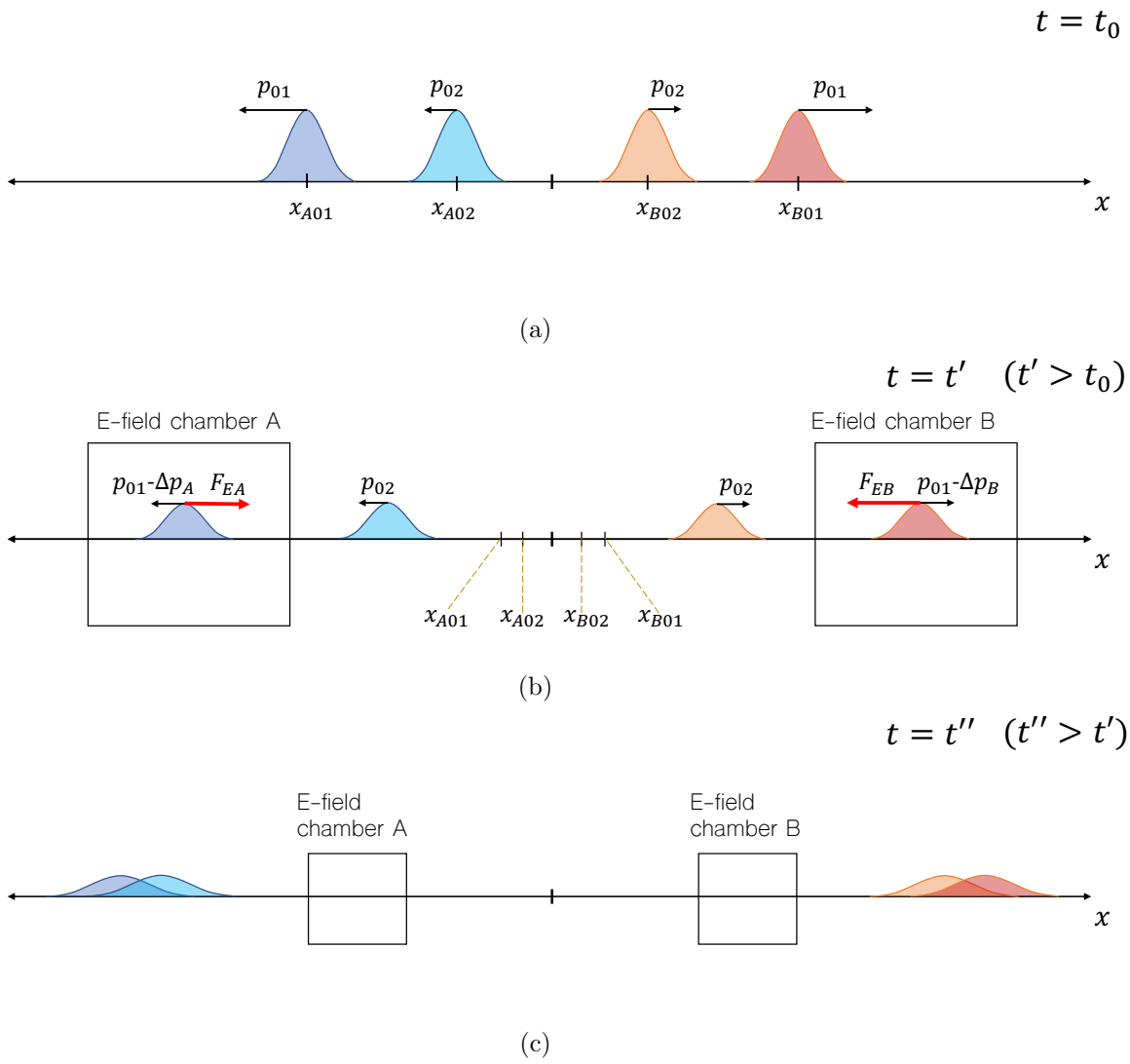

Figure 13: Illustration of the wave function at different times. Since the wave function $\Psi_{AB}(x_A,x_B,t_0)$ is entangled, it is impossible to give a representation of the individual particle states, which is why we have used the norm-square distributions $||\varphi_1(x_A,t_0)||^2$ [blue], $||\varphi_2(x_A,t_0)||^2$ [cyan], $||\tilde{\varphi}_1(x_B,t_0)||^2$ [red], $||\tilde{\varphi}_2(x_B,t_0)||^2$ [orange] to illustrate the situation. The blueish distributions are associated with particle A, the reddish distributions with B. (a) At the time $t=t_0$. The arrows represent the momenta of the maxima of the distributions. (b) At $t=t'$ $(t'>t_0)$. The high momentum wave packets $\varphi_1(x_A,t)$ and $\tilde{\varphi}_1(x_B,t)$ are within the E-field chambers, while the low momentum wave packets $\varphi_2(x_A,t)$ and $\tilde{\varphi}_2(x_B,t)$ are outside of the E-field chambers. The E-field chambers act decelerating on the wave packets $\varphi_1(x_A,t)$ and $\tilde{\varphi}_1(x_B,t)$ with forces F_{EA} and F_{EB} (red arrows), while the motion of the other two wave packets is unaltered. (c) At $t=t''$ $(t''>t')$. The distributions $||\varphi_1(x_A,t_0)||^2$ and $||\varphi_2(x_A,t_0)||^2$ as well as $||\tilde{\varphi}_1(x_B,t_0)||^2$ and $||\tilde{\varphi}_2(x_B,t_0)||^2$ overlap.

As shown in figure 13b, the experimentalists can apply a constant electric field of variable strength within specific regions of space, which we will call *E-field chambers*. It is possible to apply the E-fields in a small enough time window, such that only the wave-function components $\varphi_1(x_A, t')$ and $\tilde{\varphi}_1(x_B, t')$ are effected, while the components $\varphi_2(x_A, t')$ and $\tilde{\varphi}_2(x_B, t')$ are not altered by the E-fields, where t' ($t' > t_0$) is a time within the considered time window. It follows that at a later time t'' ($t'' > t'$) after the E-fields have been turned off again, the components $\varphi_1(x_A, t'')$ and $\varphi_2(x_A, t'')$, as well as $\tilde{\varphi}_1(x_B, t'')$ and $\tilde{\varphi}_2(x_B, t'')$ overlap (see figure 13c). By choosing E and t'' appropriately, one can achieve the special case of a perfect overlap, such that

$$\begin{aligned} ||\varphi_1(x_A, t'')||^2 &= ||\varphi_2(x_A, t'')||^2, \\ ||\tilde{\varphi}_1(x_B, t'')||^2 &= ||\tilde{\varphi}_2(x_B, t'')||^2. \end{aligned} \tag{46}$$

Conceptually, the experiment is quite similar to the DDS-experiment with a large source Ω and highly correlated momenta, which we discussed in section 2.3. By measuring whether particle B has a high or low momentum, we immediately know whether particle A has a high or low momentum and vice virsa, which is similar to the way which-slit-information about one particle implied which-slit-information about the other particle. If we express the wave function (44) symbolically as

$$|\Psi_{AB}\rangle = \frac{1}{\sqrt{2}}(|H_A\rangle\,|H_B\rangle + |L_A\rangle\,|L_B\rangle), \tag{47}$$

where H_A, L_A and H_B, L_B correspond to the possible values of O_A and O_B, equation (47) is completely analogous to equation (18) of the DDS experiment. We only have exchanged the slit-observables *right* and *left* with the momentum observables *high* and *low*.

In the DDS experiment we could decide whether we wanted to determine through which slit the particles pass or whether we would like to observe a conditional interference pattern. Similarly, in our experiment we can erase all information about whether the initial momentum of the particles was high or low by applying constant electric fields such that equation (46) is satisfied and we expect to find a conditional interference pattern, if we carry out position measurements on A and B at the time t''.

3.2 Time Evolution

3.2.1 Methods

The time evolution of the wave function (44) can be calculated with the aid of the corresponding two-particle propagator[17] $K(y_A, y_B, t; x_A, x_B, t_0)$. As we assume that A and B are not interacting for $t \geq t_0$, the propagator factorizes and we can write:

$$\Psi_{AB}(y_A, y_B, t) = \int_{-\infty}^{\infty} dx_A K(y_A, t; x_A, t_0) \int_{-\infty}^{\infty} dx_B K(y_B, t; x_B, t_0) \Psi_{AB}(x_A, x_B, t_0). \tag{48}$$

It follows that we can first calculate the individual terms

$$\begin{aligned} \varphi_j(y_A, t) &:= \int_{-\infty}^{\infty} dx_A K(y_A, t; x_A, t_0) \varphi_j(x_A, t_0), \\ \tilde{\varphi}_j(y_B, t) &:= \int_{-\infty}^{\infty} dx_B K(y_B, t; x_B, t_0) \tilde{\varphi}_j(x_B, t_0) \end{aligned} \tag{49}$$

and then assembly the wave function $\Psi_{AB}(y_A, y_B, t)$ from these individual terms, such that

$$\Psi_{AB}(y_A, y_B, t) = \frac{1}{\sqrt{2}} \Big\{ \varphi_1(y_A, t) \tilde{\varphi}_1(y_B, t) + \varphi_2(y_A, t) \tilde{\varphi}_2(y_B, t) \Big\}. \tag{50}$$

For the free particle (F) and a charged particle in a constant electric field (E) the propagators are given by[18]:

$$K_F(y, t_1; x, t_0) = \sqrt{\frac{m}{2\pi\hbar i \Delta t}} \exp\Big(\frac{i}{\hbar} \frac{m(y-x)^2}{2\Delta t} \Big), \tag{51}$$

$$K_E(y, t_1; x, t_0) = \sqrt{\frac{m}{2\pi\hbar i \Delta t}} \exp\Big(\frac{i}{\hbar} \Big\{ \frac{m(y-x)^2}{2\Delta t} + \frac{F\Delta t(y+x)}{2} - \frac{1}{24} F^2 \Delta t^3 \Big\} \Big), \tag{52}$$

where m is the mass of the particle. It turns out that for a gaussian wave packet of the form

$$\varphi(x) = (2\pi\sigma_0^2)^{-1/4} \exp\Big(- \frac{(x-x_0)^2}{4\sigma_0^2} \Big) \exp\Big(- i \frac{p_0}{\hbar} (x - x_0) \Big), \tag{53}$$

the group velocity of the packet coincides (for the free particle as well as for the particle in the constant electric field) with the velocity of a classical particle. The classical velocities for a free particle (v_F) and a particle in a constant electric field (v_E) are

[17] The propagator and its basic properties are introduced in the Appendix 5.3.

[18] These expressions are derived in the Appendix 5.3

given by:

$$v_F = \frac{p_0}{m}, \qquad v_E = \frac{qE}{m}\Delta t + \frac{p_0}{m}, \tag{54}$$

where m is the mass of the particle and q the charge. In both cases the spread of the packets is determined by:

$$\sigma(\Delta t) = \sigma_0 \sqrt{1 + \frac{\hbar^2 \Delta t^2}{4m^2\sigma_0^4}}. \tag{55}$$

For our calculation we are only considering such cases, where for the whole time interval during which the E-field chambers produce an electric field, the maxima of the small momentum wave packets ($\varphi_2(y_A, t)$ and $\tilde{\varphi}_2(y_B, t)$) are more than $3\sigma(\Delta t)$ away from the E-field chambers, while the maxima of the high momentum wave packets ($\varphi_1(y_A, t)$ and $\tilde{\varphi}_1(y_B, t)$) are within the chambers and more than $3\sigma(\Delta t)$ away from the field-free outer space. We consider the following order of events:

1. *At t_0 the initial state is given by* (44).
2. *At t_1 the E-field chambers are turned on.*
3. *At t_2 the E-field chambers are turned off.*
4. *At t_3 the final position measurement is carried out.*

Then, the wave function $\Psi_{AB}(w_A, w_B, t_3)$ can be assembled according to equation (50) from the individual terms:

$$\begin{aligned}
\varphi_1(w_A, t_3) = &\int_{-\infty}^{\infty} dz_A K_F(w_A, t_3; z_A, t_2) \int_{-\infty}^{\infty} dy_A K_E(z_A, t_2; y_A, t_1) \cdot \\
&\int_{-\infty}^{\infty} dx_A K_F(y_A, t_1; x_A, t_0) \varphi_1(x_A, t_0), \\
\varphi_2(w_A, t_3) = &\int_{-\infty}^{\infty} dx_A K_F(w_A, t_3; x_A, t_0) \varphi_2(x_A, t_0), \\
\tilde{\varphi}_1(w_B, t_3) = &\int_{-\infty}^{\infty} dz_B K_F(w_B, t_3; z_B, t_2) \int_{-\infty}^{\infty} dy_B K_E(z_B, t_2; y_B, t_1) \cdot \\
&\int_{-\infty}^{\infty} dx_B K_F(y_B, t_1; x_B, t_0) \tilde{\varphi}_1(x_B, t_0), \\
\tilde{\varphi}_2(w_B, t_3) = &\int_{-\infty}^{\infty} dx_B K_F(w_B, t_3; x_B, t_0) \tilde{\varphi}_2(x_B, t_0).
\end{aligned} \tag{56}$$

It has been proven to be useful for the numerical evaluation of the integrals to rewrite the integral transforms in terms of a Fourier-transform ($\mathcal{F}$) and a subsequent back-transform ($\mathcal{F}^{-1}$). This allows the implementation of fast-Fourier-transforms (FFTs) in

the numerical integration. We find that[19]

$$\begin{aligned}\varphi_j(y_A,t) &= \mathcal{F}^{-1}\Big\{\exp\Big(-i\hbar\frac{k^2}{2m_A}\Delta t\Big)\mathcal{F}(\varphi_j(x_A,t_0))\Big\},\\ \tilde{\varphi}_j(y_B,t) &= \mathcal{F}^{-1}\Big\{\exp\Big(-i\hbar\frac{k^2}{2m_B}\Delta t\Big)\mathcal{F}(\tilde{\varphi}_j(x_B,t_0))\Big\}\end{aligned} \tag{57}$$

for the free particle propagator and

$$\begin{aligned}\varphi_j(y_A,t) &= g(\Delta t)\mathcal{F}^{-1}\Big\{\exp\Big(-i\Big[\frac{F}{m_A}k\Delta t^2+\hbar\frac{k^2}{2m_A}\Delta t\Big]\Big)\mathcal{F}\Big\{\exp\Big(-\frac{i}{2\hbar}xF\Delta t\Big)\varphi_j(x_A,t_0))\Big\}\Big\},\\ \tilde{\varphi}_j(y_B,t) &= g(\Delta t)\mathcal{F}^{-1}\Big\{\exp\Big(-i\Big[\frac{F}{m_B}k\Delta t^2+\hbar\frac{k^2}{2m_B}\Delta t\Big]\Big)\mathcal{F}\Big\{\exp\Big(-\frac{i}{2\hbar}xF\Delta t\Big)\tilde{\varphi}_j(x_B,t_0))\Big\}\Big\}\end{aligned} \tag{58}$$

for the constant E-field propagator, where $g(\Delta t)$ is given by:

$$g(\Delta t) = \exp\Big(\frac{i}{\hbar}\Big[\frac{3}{2}yF\Delta t - \frac{13}{24m}F^2\Delta t^3\Big]\Big). \tag{59}$$

We can thus determine the wave function $\Psi_{AB}(x_A,x_B,t_3)$ by means of the algorithm of figure 14. From $\Psi_{AB}(x_A,x_B,t_3)$ we can determine the probability

$$P(x_A,x_B,t_3) := ||\Psi_{AB}(x_A,x_B,t_3)||^2, \tag{60}$$

which is the probability to find A at x_A and B at x_B at the time t_3. The single particle probabilities $P(x_A,t_3)$ and $P(x_B,t_3)$ to find A at x_A at t_3 and to find B at x_B at t_3 are given by:

$$\begin{aligned}P(x_A,t_3) &= \int_{-\infty}^{\infty} dx_B P(x_A,x_B,t_3),\\ P(x_B,t_3) &= \int_{-\infty}^{\infty} dx_A P(x_A,x_B,t_3)\end{aligned} \tag{61}$$

and the conditional probabilities $P(x_A,t_3|x_B,t_3)$ to find A at x_A at t_3 under the condition that B is found at x_B at t_3 and $P(x_B,t_3|x_A,t_3)$ to find B at x_B at t_3 under the condition that A is found at x_A at t_3 are given by:

$$P(x_A,t_3|x_B,t_3) = \frac{P(x_A,x_B,t_3)}{P(x_B,t_3)}, \qquad P(x_B,t_3|x_A,t_3) = \frac{P(x_A,x_B,t_3)}{P(x_A,t_3)}. \tag{62}$$

[19] See Appendix 5.3

3.2.2 Algorithm

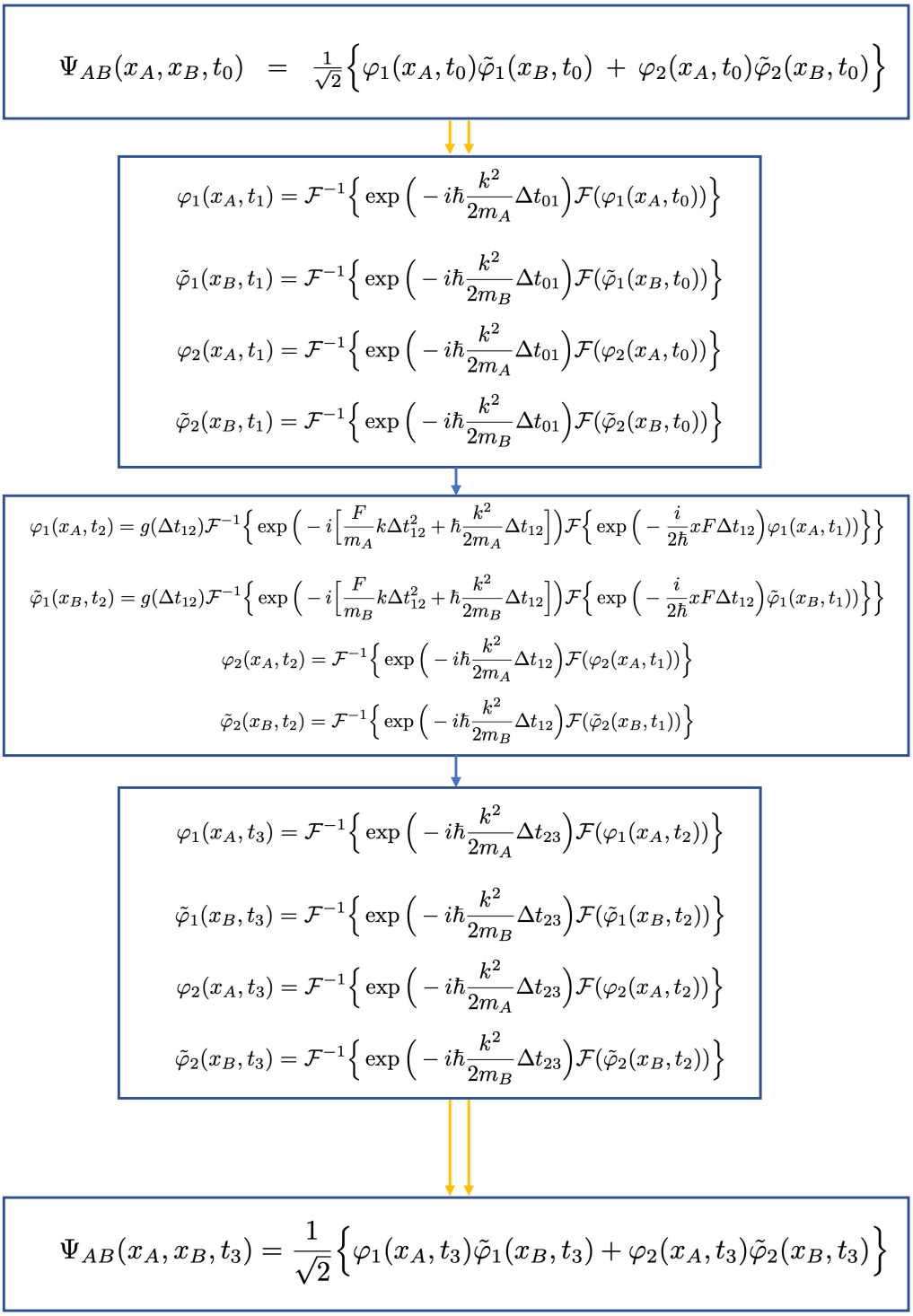

Figure 14: Algorithm for the determination of $\Psi_{AB}(x_A, x_B, t_3)$.

3.3 Interference

For illustration purposes, we numerically evaluated our algorithm using the parameters

$m_A = m_B = m_e = 9.1094 \cdot 10^{-31}\,\text{kg}$,
$\sigma_0 = 10\,\mu\text{m}$,
$x_{A01} = -x_{B01} = -100\,\mu\text{m}$,
$x_{A02} = -x_{B02} = -100\,\mu\text{m}$,
$k_{01} = 3.25 \cdot k_{02} = -0.52\,\frac{1}{\mu\text{m}}$,
$t_0 = 0$, $t_1 = 2 \cdot 10^{-5}\,\text{s}$,
$t_2 = 2.04 \cdot 10^{-5}\,\text{s}$,
$t_3 = 8.14 \cdot 10^{-5}\,\text{s}$,

where t_1 is the time the E-fields are turned on, t_2 the time the E-fields are tuned off and t_3 the time of a position measurement on particle A and B (see also the previous section 3.2). As we have already seen in figure 12, these values assure that the momentum observables O_A and O_B with the possible values H and L can be unambiguously defined. The time interval $\Delta_{12} = |t_2 - t_1| = 4 \cdot 10^{-7}\,\text{s}$ for which the E-field chambers are turned on, has been chosen to be rather small for computational convenience. As we will see, this implies high E-field values, which might be difficult to achieve in real experiments. However, none of our results depends on this particular choice. All results could be produced with significantly lower E-fields, which are applied over a longer period of time. For convenience, we have also set $x_{A01} = x_{A02}$ and $x_{B01} = x_{B02}$ and assumed that A and B have the same mass m_e.
By setting the E-fields to $E = 803.605\,\frac{\text{V}}{\mu\text{m}}$, we satisfy equation (46) for the time t_3, leading to

$$\begin{aligned} ||\varphi_1(x_A, t_3)||^2 &= ||\varphi_2(x_A, t_3)||^2, \\ ||\tilde{\varphi}_1(x_B, t_3)||^2 &= ||\tilde{\varphi}_2(x_B, t_3)||^2. \end{aligned} \tag{63}$$

If we now consider the two-particle position distribution $||\Psi_{AB}(x_A, x_B, t_3)||^2$ for position measurements at t_3, we obtain the perfect two-particle interference pattern of figure 15.
The fringes of the interference pattern run at a 45° diagonal such that when they are sliced vertically (fixed A-position) we obtain a conditional B-interference pattern and when they are sliced horizontally (fixed B-position) we obtain a conditional A-interference pattern. It has to be kept in mind that neither the A-position distribution $P(x_A)$ nor the B-position distribution $P(x_B)$ shows any interference. They are stan-

dard gaussian distributions. Only by considering the appropriate data-subsets, the interference becomes visible.

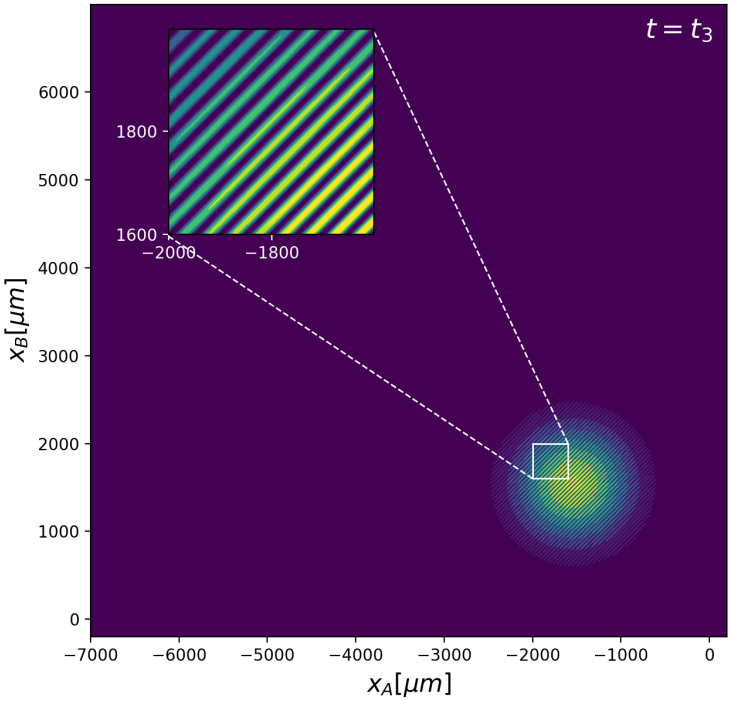

Figure 15: Density plot of position distribution $P(x_A, x_B, t_3) = ||\Psi_{AB}(x_A, x_B, t_3)||^2$.

In figure 16 we have plotted a conditional A-interference pattern for the fixed B-position $x_{B1} = 1538\,\mu\text{m}$. The gaussian shape blue curve represents what we would obtain, if we would measure for each particle whether it has a high or a low momentum *before* the electric fields are applied to the system. It corresponds essentially to what we would classically expect, if each particle either had a high or a low momentum.
By setting the electric fields of the A-chamber and B-chamber to different values, e.g. $E_A = 803.605\,\frac{\text{V}}{\mu\text{m}}$ and $E_B = 500\,\frac{\text{V}}{\mu\text{m}}$, we can regain partial information about the initial momenta of the particles and in analogy with the DDS-experiment, we obtain an interference pattern with a reduced visibility[20]. This is illustrated in figure 17.

[20]The interference pattern does not only have a reduced visibility, it also becomes unsymmetrical in dependence of the difference between the two E-fields $E_A - E_B$.

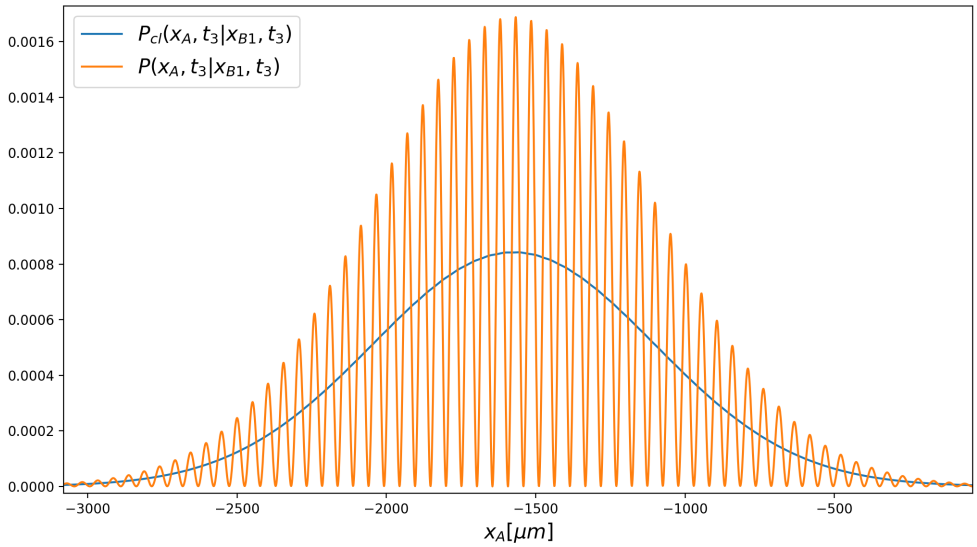

Figure 16: Position distribution $P(x_A, x_{B1}, t_3) = ||\Psi_{AB}(x_A, x_{B1}, t_3)||^2$. The electric field-strengths are set to $E_A = E_B = 803.605\,\frac{\mathrm{V}}{\mu\mathrm{m}}$. The fixed B-position is given by $x_{B1} = 1538\,\mu\mathrm{m}$.

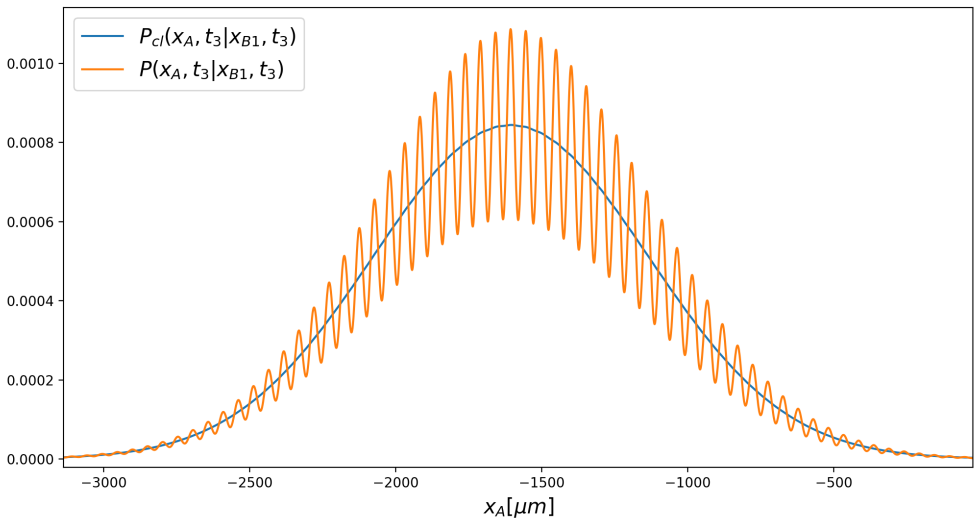

Figure 17: Position distribution $P(x_A, x_{B1}, t_3) = ||\Psi_{AB}(x_A, x_{B1}, t_3)||^2$ with $E_A = 803.605\,\frac{\mathrm{V}}{\mu\mathrm{m}}$ and $E_B = 500\,\frac{\mathrm{V}}{\mu\mathrm{m}}$. The fixed B-position is given by $x_{B1} = 1538\,\mu\mathrm{m}$.

3.4 An Analogy

In order to tackle Bell's theorem by means of our experimental arrangement, we will focus solely on the E-field configuration, which satisfies (46), where no information about whether the initial particle momentum was high or low is present. We can determine the period T of the interference pattern in figure 16 by dividing the distance between two distant interference maxima by the number of cycles between the two maxima. We obtain $T = 51.83\,\mu\text{m}$. For the A-interference pattern in figure 16 we chose the point $x_{B1} := 1538\,\mu\text{m}$ as fixed B-point. If we choose a different point we will obtain a shifted A-interference pattern with the same period. If we set, for example, $x_{B4} := x_{B1} + T/2$, we obtain the *anti-fringes* to the interference pattern in figure 16, i.e. maxima are shifted to minima and minima to maxima (see figure 18).

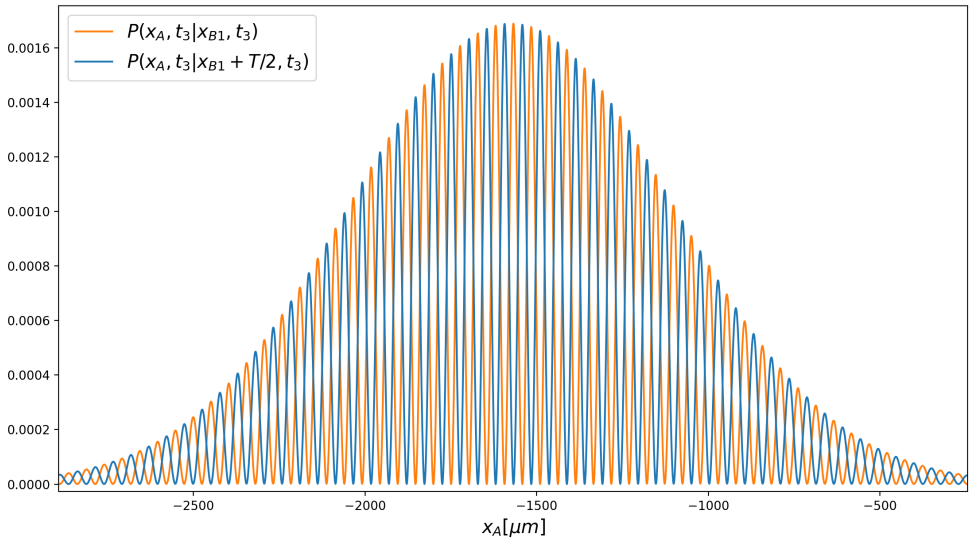

Figure 18: Fringes of $P(x_A, t_3|x_{B1}, t_3)$ [orange] and and anti-fringes of $P(x_A, t_3|x_{B4}, t_3)$ [blue], whereas x_{B4} is defined by $x_{B4} := x_{B1} + T/2$.

But we can also switch the roles by considering B-interference patterns for fixed A-positions. If we call one of the central maxima of the A-interference in figure 16 x_{A1} ($x_{A1} = -1515.82\,\mu\text{m}$) and define $x_{A4} := x_{A1} + T/2$, we can also consider the two B-interference patterns for x_{A1} and x_{A4} respectively. As can be seen in figure 19, where we have zoomed into the B-interference patterns, one finds again fringes and anti-fringes and the maxima (minima) of the interference patterns coincide with our previously considered fixed B-points x_{B1} and x_{B4}!

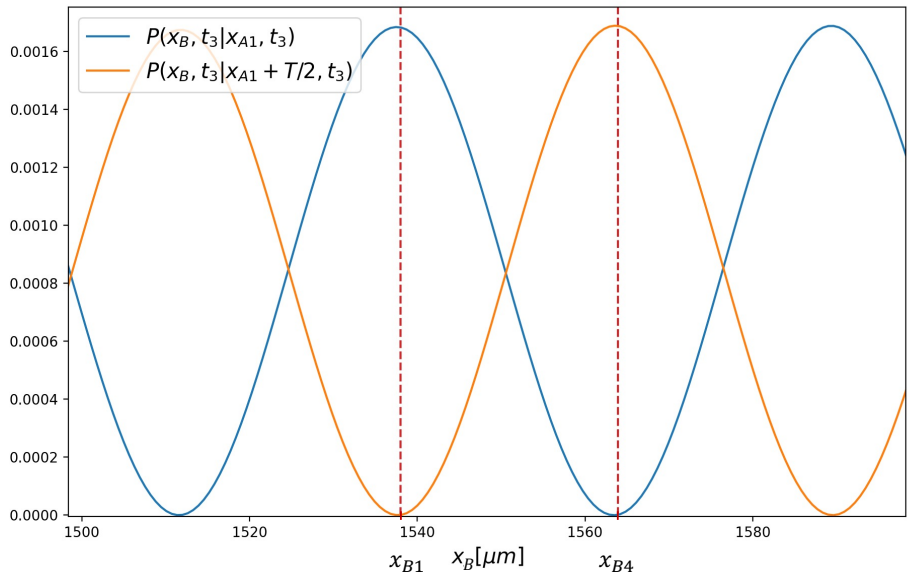

Figure 19: Position distributions $P(x_B, t_3|x_{A1}, t_3)$ [blue] and $P(x_B, t_3|x_{A4}, t_3)$ [orange]. The values x_{B1} and x_{B4} are marked by red dashed lines.

From this follows our first observation:

Observation 1:
If we consider only those runs, where A is found at x_{A1} or x_{A4} and B is found at x_{B1} or x_{B4}:
If A is found at x_{A1}, B is found at x_{B1} and vice virsa.
If A is found at x_{A4}, B is found at x_{B4} and vice virsa.

This observation follows from the fact that if e.g. particle A is found at x_{A1} the B-interference will have a maximum at x_{B1} and a minimum (equal to zero!) at x_{B4}. Thus particle B must be found at x_{B1} and so on.
We can obviously also consider other pairs of points, which are seperated by $T/2$ and could make the same observation. If we define, for example, the points x'_{A1}, x'_{A4} by (see figure 20):

$$\begin{aligned} x'_{A1} &= x_{A1} + \frac{T}{4}, \\ x'_{A4} &= x_{A4} + \frac{T}{4} = x_{A1} + \frac{3T}{4} \end{aligned} \tag{64}$$

and the points x'_{B1}, x'_{B4} by (see figure 21):

$$\begin{aligned} x'_{B1} &= x_{B1} + \frac{T}{4}, \\ x'_{B4} &= x_{B4} + \frac{T}{4} = x_{B1} + \frac{3T}{4}, \end{aligned} \tag{65}$$

x'_{A1} and x'_{A2} as well as x'_{B1} and x'_{B4} are separated by $T/2$ and observation 1 holds true for the points $x'_{A1}, x'_{A4}, x'_{B1}, x'_{B4}$.

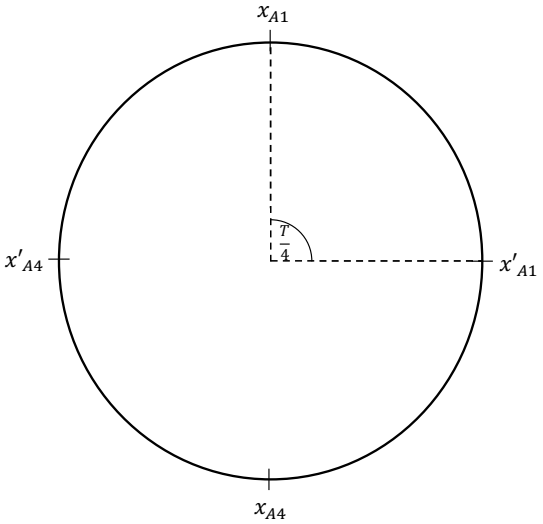

Figure 20: The points $x_{A1}, x_{A4}, x'_{A1}, x'_{A4}$ placed on a circle with $2\pi \equiv T$.

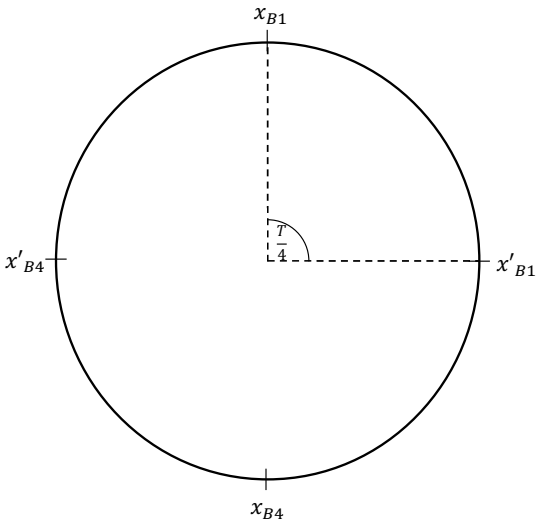

Figure 21: The points $x_{B1}, x_{B4}, x'_{B1}, x'_{B4}$ placed on a circle with $2\pi \equiv T$.

However, what happens, if we consider e.g. the points $x_{A1}, x_{A4}, x'_{B1}, x'_{B4}$? Mathematically, the probability[21]:

$$P_{\alpha_1}(x_{A1}|x'_{B1}) := \frac{P(x_{A1}, t_3|x'_{B1}, t_3)}{P(x_{A1}, t_3|x'_{B1}, t_3) + P(x_{A4}, t_3|x'_{B1}, t_3)} \tag{66}$$

gives the conditional probability that A is found at x_{A1} under the condition that B is found at x'_{B1} *and* that A is found either at x_{A1} or x_{A4}. Some care has to be taken here, since the probability to find an event at an exact position is zero. However, from an experimental point of view one would consider a grid with small bins and make the calculation for each bin of the grid, which agrees with our numerical approach and which is how all considered events should be understood. We can thus consider the

[21] Our terminology with the α_1 in $P_{\alpha_1}(x_{A1}|x'_{B1})$ will become clear in the next section.

four probabilities $P_{\alpha_1}(x_{A1}|x'_{B1})$, $P_{\alpha_1}(x_{A1}|x'_{B4})$, $P_{\alpha_1}(x_{A4}|x'_{B1})$ and $P_{\alpha_1}(x_{A4}|x'_{B4})$. As can be seen from figure 22, where we have plotted the A-interference patterns for fixed points x'_{B1} and x'_{B4} and marked x_{A1} and x_{A4} by blue dashed lines, it holds that

$$P_{\alpha_1}(x_{A1}|x'_{B1}) = P_{\alpha_1}(x_{A1}|x'_{B4}) = P_{\alpha_1}(x_{A4}|x'_{B1}) = P_{\alpha_1}(x_{A4}|x'_{B4}) = \frac{1}{2}. \tag{67}$$

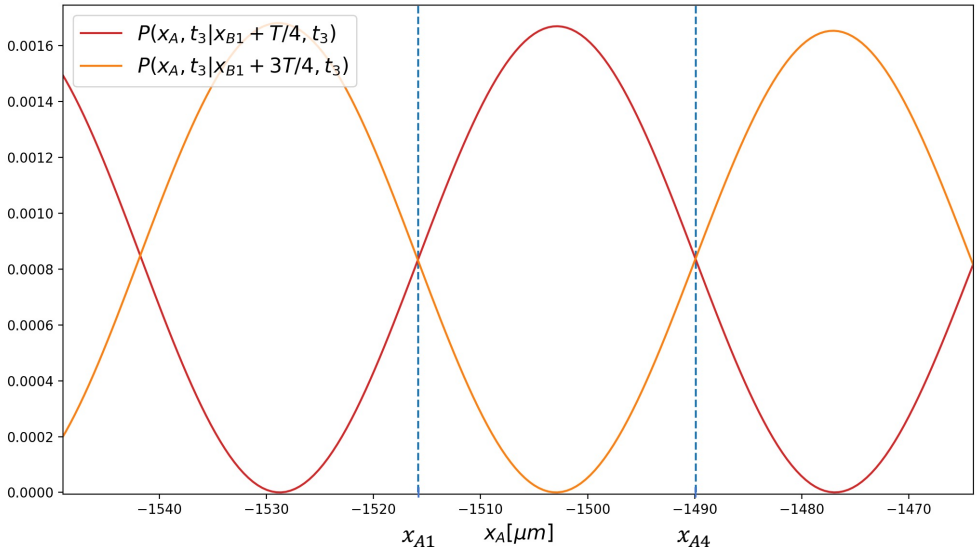

Figure 22: Position distributions $P(x_A, t_3|x'_{B1}, t_3)$ [red], $P(x_A, t_3|x'_{B4}, t_3)$ [orange]. The values x_{A1} and x_{A4} are marked by blue dashed lines.

And if we would reverse the roles of A and B, we would naturally obtain the same result. This leads us to our second observation:

Observation 2:
If we only consider those runs, where A is found at x_{A1} or x_{A4} and B is found at x'_{B1} or x'_{B4}:
If A is found at x_{A1}, B is equally likely to be found at x'_{B1} and x'_{B4}.
If A is found at x_{A4}, B is equally likely to be found at x'_{B1} and x'_{B4}.
If B is found at x'_{B1}, A is equally likely to be found at x_{A1} and x_{A4}.
If B is found at x'_{B4}, A is equally likely to be found at x_{A1} and x_{A4}.

Let us now consider a pair of spin-$\frac{1}{2}$ particles in the singlet-state. For particle A

let us call the *spin-up* and *spin-down* along the x-axis x_{A1} and x_{A4} and along the y-axis x'_{A1} and x'_{A4}. For particle B let us call the *spin-up* and *spin-down* along the x-axis x_{B4} and x_{B1} and along the y-axis x'_{B4} and x'_{B1}. With this terminology we see that the pair of spin-$\frac{1}{2}$ particles in the singlet-state reproduces *exactly* the observations 1 and 2, whereas observation 1 corresponds to measurements along the same axis (x-axis), and observation 2 to measurements along orthogonal axis (x and y-axis).
In analogy to the spin-$\frac{1}{2}$ particle, we can thus arrange all points x_A, x_B lying in the intervals $[x_{A1}, x_{A1}+T)$ and $[x_{B1}, x_{B1}+T)$ on the circles in figure 20 and 21 and it is to be expected that all predictions for two spin-$\frac{1}{2}$ particles in the singlet state, which are measured along an arbitrary axis in the xy-plane, are reproduced in our experiment.

3.5 Bell's Theorem from Quantum Interference

3.5.1 The Setting

In Mermin's prove of Bell's theorem we considered three A-measurement configurations, $\alpha_1, \alpha_2, \alpha_3$ and three B-measurement configurations $\beta_1, \beta_2, \beta_3$. In our experiment, we will say that the configuration α_1 is present, whenever A is found at either[22] x_{A1} or x_{A4}. In most repetitions of the experiment, this will not be the case, since the A-particle will be found at some other location x_A. However, every now and then the particle will be found at x_{A1} or x_{A4} and always, when this happens, it will be said that the *measurement configuration* was α_1 and that the *measurement result* was $0[\alpha_1]$, if A was found at x_{A1} and $1[\alpha_1]$, if A was found at x_{A4} (see figure 23). By further making the definitions:

$$\begin{aligned} x_{A2} &:= x_{A1} + \frac{T}{6}, & x_{A3} &:= x_{A1} + \frac{T}{3}, \\ x_{A5} &:= x_{A1} + \frac{2T}{3}, & x_{A6} &:= x_{A1} + \frac{5T}{6}, \end{aligned} \tag{68}$$

we can say that the configuration α_2 is present, whenever A is found at x_{A3} or x_{A6} and that the configuration α_3 is present, whenever A is found at x_{A5} or x_{A2}. Furthermore, we will say that the measurement outcome is $0[\alpha_2]$, if A is found at x_{A3}, and $1[\alpha_2]$, if A is found at x_{A6}, and that measurement outcome is $0[\alpha_3]$, if A is found at x_{A5}, and $1[\alpha_3]$, if A is found at x_{A2} (see figure 23).

[22] Again, the positions x_{A1} and x_{A4} are understood as small bins in a position grid.

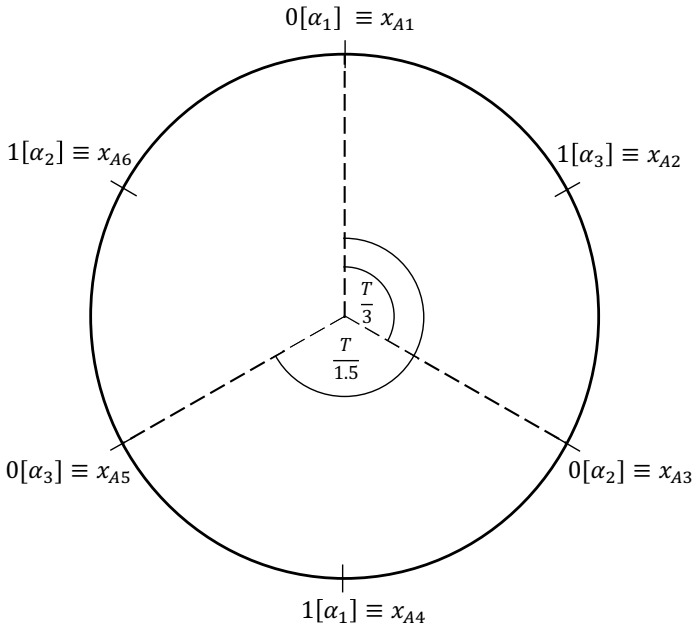

Figure 23: Possible measurement settings and measurement results: Opposite points on the circle belong to the same measurement configuration and represent different possible measurement results.

Similarly, we can define the configurations $\beta_1, \beta_2, \beta_3$ and the corresponding measurement results. We now see that the probability $P_{\alpha_1}(x_{A1}|x_B)$ in (66) is the conditional probability to find A at x_{A1} under the condition that B is found at x_B and that the configuration is α_1. In the same way, we can e.g. define the probabilities $P_{\alpha_2}(x_{A3}|x_B)$ and $P_{\alpha_3}(x_{A5}|x_B)$ by the equations

$$\begin{aligned} P_{\alpha_2}(x_{A3}|x_B) &:= \frac{P(x_{A3}, t_3|x_B, t_3)}{P(x_{A3}, t_3|x_B, t_3) + P(x_{A6}, t_3|x_B, t_3)}, \\ P_{\alpha_3}(x_{A5}|x_B) &:= \frac{P(x_{A5}, t_3|x_B, t_3)}{P(x_{A5}, t_3|x_B, t_3) + P(x_{A2}, t_3|x_B, t_3)}. \end{aligned} \tag{69}$$

The probability $P(\alpha_1)$ that the configuration α_1 is present, is given by:

$$P(\alpha_1) = P(x_{A1}) + P(x_{A4}). \tag{70}$$

Since we have chosen the values $x_{A1} - x_{A6}$ and $x_{B1} - x_{B6}$ such that they all lie in a small neighborhood around the maximum of the gaussian distributions $P(x_A, t_3)$ and

$P(x_B, t_3)$, we can state to a good approximation that

$$\begin{aligned} P(\alpha_1) = P(\alpha_2) = P(\alpha_3), \\ P(\beta_1) = P(\beta_2) = P(\beta_3). \end{aligned} \tag{71}$$

Equation (71) says that all measurement configurations occur with the same likelihood, which agrees with the setting in Mermin's proof. However, while in Mermin's proof there is an external agent, who freely chooses a specific measurement configuration, in our experiment the configuration is directly generated by the quantum process under consideration. As we will see in section 3.5.3, this difference to Mermin's original proposal is significant.
We also note that in our experiment no event γ exists, such that the probabilities $P(\alpha_i|\gamma)$ and $P(\beta_i|\gamma)$ are equal to 0 or 1. According to our discussion about determinism in section 2.10 this suggests that the events $\alpha_1, \alpha_2, \alpha_3, \beta_1, \beta_2, \beta_3$ are inherently indeterministic. We will return to this observation in sections 3.5.3 and 4.
By adapting Mermin's phrasing of the setting in terms of detectors D_A and D_B, which can flash two different lights associated with the outcomes 0 and 1, we can formulate in analogy to section 2.8 the following two predictions:

- If the settings of D_A and D_B are the same, i.e. if $i = j$ for α_i and β_j, the results of the two measurers always *agree*, i.e. whenever D_A flashes the 0-light, D_B flashes the 0-light and whenever D_A flashes the 1-light, D_B flashes the 1-light.
- If one considers an *arbitrary* run of the experiment, the probability $P(+)$ that D_A and D_B flash the *same* light is given by $P(+) = \frac{1}{2}$.

Note that while in Mermin's prove in section 2.8 the first feature expressed a perfect *anti-correlation*, we are now considering a perfect *correlation*. If we can show that the quantum mechanical prediction for our experiment reproduces these two features and that the local HV prediction does not, we have proven Bell's theorem in the context of our experiment.

3.5.2 The Quantum Mechanical Point of View

We have already proven in section 3.4 that the first feature is fulfilled (this was observation 1). So we need only to show that the second feature is fulfilled as well. In analogy to section 2.8.2, we will consider the individual case that for particle B we

find $0[\beta_2] \equiv x_{B3}$ and generalize from there. In figure 24 we see the A-interference pattern for fixed position x_{B3}. We have indicated x_{A1} $(0[\alpha_1])$ and x_{A4} $(1[\alpha_1])$ by blue dashed lines (configuration α_1) and x_{A5} $(0[\alpha_3])$ and x_{A2} $(1[\alpha_3])$ by green dashed lines (configuration α_3). One can see that

$$P_{\alpha_1}(x_{A1}|x_{B3}) = P_{\alpha_3}(x_{A5}|x_{B3}) \tag{72}$$

by noting that the red line of the interference pattern crosses the blue dashed line to the left of the figure (indicating x_{A1}) at the same y-value as it crosses the green dashed line to the right of the figure (indicating x_{A5}).

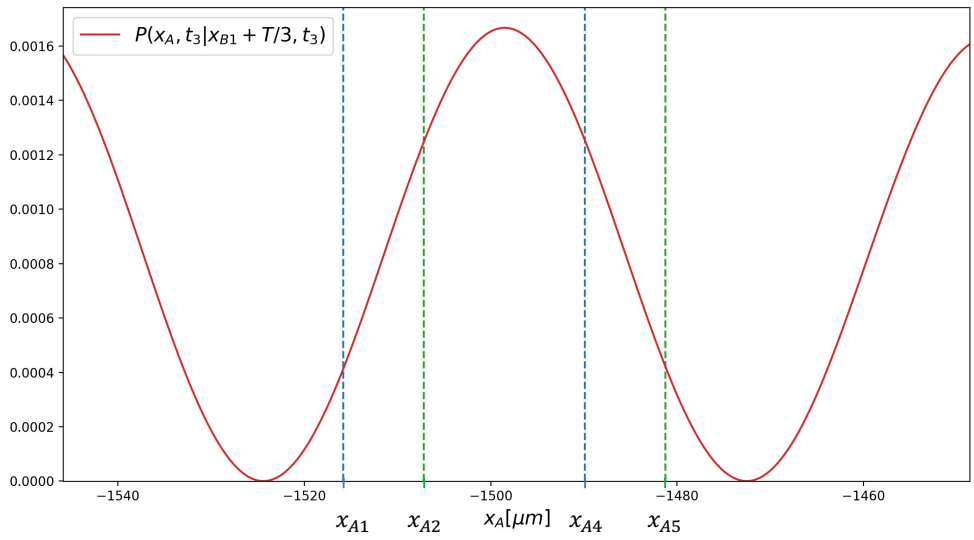

Figure 24: Position distribution $P(x_A, t_3|x_{B3}, t_3)$: x_{A1} and x_{A4} are indicated by blue dashed lines and x_{A5} and x_{A2} by green dashed lines.

The calculation yields

$$P_{\alpha_1}(x_{A1}|x_{B3}) = P_{\alpha_3}(x_{A5}|x_{B3}) = \frac{1}{4}. \tag{73}$$

According to our identification in figure 23 this is equivalent to

$$P\big(0[\alpha_1]\big|0[\beta_2]\big) = P\big(0[\alpha_3]\big|0[\beta_2]\big) = \frac{1}{4}. \tag{74}$$

Equation (74) states that the probability that D_A flashes the 0-light in the configuration

α_1 under the condition that D_B flashes the 0-light in the configuration β_2 is equal to 1/4 and similarly for the configuration α_3. Since all of our configurations $\alpha_1, \alpha_2, \alpha_3$ are equally likely, it follows that

$$\begin{aligned} P\big(0\big|0[\beta_2]\big) &= \frac{1}{3}\Big\{P\big(0[\alpha_1]\big|0[\beta_2]\big) + P\big(0[\alpha_2]\big|0[\beta_2]\big) + P\big(0[\alpha_3]\big|0[\beta_2]\big)\Big\} \\ &= \frac{1}{3}(\frac{1}{4} + 1 + \frac{1}{4}) = \frac{1}{2}. \end{aligned} \tag{75}$$

By repeating the calculation for β_1 and β_3, we obtain the same result and thus conclude that $P(0_A|0_B) = 1/2$. Carrying out the same calculation for $P(1_A|1_B)$ we also find that $P(1_A|1_B) = 1/2$ and from equation (29), which we have introduced in section 2.8, we obtain:

$$P(+) = P(0_A|0_B)P(0_B) + P(1_A|1_B)P(1_B) = \frac{1}{2}(P(0_B) + P(1_B)) = \frac{1}{2} \tag{76}$$

Equation (76) proves that the quantum mechanical predictions necessary for Mermin's proof of Bell's theorem are reproduced in the context of our experiment.

3.5.3 The Hidden Variables Point of View

In Mermin's proof of Bell's theorem in section 2.8.3, we considered instruction sets, which determined the values for *all three* measurement configurations $\alpha_1, \alpha_2, \alpha_3$ (β_1, β_2, β_3). By considering the statistics for these three-valued instruction sets, we derived the inequality $P(+) < \frac{4}{9}$, which is violated by the quantum mechanical prediction $P(+) = 1/2$.

We came to the conclusion that local HV theories necessarily imply three-valued instruction sets on the basis of the three assumptions: parameter independence, outcome independence and statistical independence (see section 2.9). Parameter independence taken together with outcome independence was called factorability. In our experiment factorability amounts to the assumption that

$$P_{\alpha_l}(x_{Ai}|\lambda, x_{Bj}) = P_{\alpha_l}(x_{Ai}|\lambda), \tag{77}$$

which says that the location, where particle A is detected, does not depend on the location, where particle B is detected. Because x_{Bj} and x_{Ai} are determined at the same time t_3, the A and B-measurement events are space-like separated, such that the B-value x_{Bj} (which also determines the measurement configuration β_k) can not have

any influence on the A-value x_{Ai}. We thus conclude that parameter independence and outcome independence are satisfied in the context of our experiment. It remains to show that statistical independence is fulfilled as well.

However, as was already foreshadowed in section 3.5.1, statistical independence takes on quite a different appearance than in Mermin's proofs of Bell's theorem. As we have discussed in section 2.9, statistical independence is a plausibility assumption, which is based on the apparent independence of the observer, who determines the measurement-configuration, and the particle, which is being observed. But since in our experiment the measurement configuration is generated by the particle itself, this independence is lost and without any additional argument statistical independence can not be assumed.

But if statistical independence is not a justified assumption in our experiment, the measurement configurations α, β could depend on the hidden variables λ, such that $\alpha = \alpha(\lambda)$ and $\beta = \beta(\lambda)$, and it would be possible to account for the two features of the quantum mechanical data by assuming for example the existence of two-valued instruction sets for each particle, where one value determines the measurement configuration and the other value the measurement outcome. But then the reasoning of section 2.8.3 brakes down and the inequality $P(+) < \frac{4}{9}$ can not be derived. We thus see that the loss of independence between the entity, which determines the measurement-configuration, and the entity, which is being observed, undermines the plausibility of statistical independence and thereby overthrows our attempted proof of Bell's Theorem.

However, the situation changes completely, if the events α_i, β_j are inherently indeterministic: According to our definition of inherently indeterministic events in section 2.10 an event a_i is inherently indeterministic, *if there exist no elements of reality, which could be represented by hidden variables λ, such that λ determines whether a_i is found or not, i.e. such that $P(a_i|\alpha_i, \lambda)$ is equal to zero or one.* Thus, if α_i, β_j are inherently indeterministic events, they can not be encoded in the HVs λ and in effect local HV theories must specify at least three-valued instruction sets in order to reproduce the first feature of the quantum mechanical data[23]. But then, also the reasoning of section 2.8.3, which led to the inequality $P(+) < \frac{4}{9}$ and thereby to the proof of Bell's Theorem, can be fully adopted.

As we have already mentioned in section 3.5.1, the argumentation in section 2.10 indeed suggests that the events α_i, β_j are inherently indeterministic. However, as we will discuss in some detail in section 4, the argumentation as it stands is not sufficient.

[23]See section 2.8.3 for a remainder of the connection between three-valued instruction sets and the first feature of the quantum mechanical data.

3.6 Experimental Variation

Our experimental scheme was based on perfect position measurements: *At t_3 the particle is found somewhere.* It might be rather difficult to implement such measurements experimentally. More realistically would be a scenario, where two detectors are placed at the fixed locations x_{DA} and x_{DB} on opposite sites of the source, as it would e.g. be the case with a reaction microscope (ReMi) [55]. For this set-up, rather than considering the x_A and x_B dependent distribution $P(x_A, t_3|x_B, t_3)$, one would like to calculate the distribution $P(x_{DA}, t|x_{DB}, t')$ to find the particle A at x_{DA} at the time t under the condition that the particle B is found at x_{DB} at the time t', as a function of t and t'. A *necessary* condition to adopt our previous argumentation to that case is that the *spatial* two particle interference extends to a *temporal* two particle interference, if the time of arrival (TOA) at a fixed detector location is measured. That this condition is fulfilled can be seen in figure 25, where we have plotted the probability density $||\Psi_{AB}((x_{DA}, t), (x_{DB}, t'))||^2$ with $\Psi_{AB}((x_{DA}, t), (x_{DB}, t'))$ being given by:

$$\Psi_{AB}((x_A, t), (x_B, t')) = \frac{1}{\sqrt{2}}\Big\{\varphi_1(x_A, t)\tilde{\varphi}_1(x_B, t') + \varphi_2(x_A, t)\tilde{\varphi}_2(x_B, t')\Big\}. \tag{78}$$

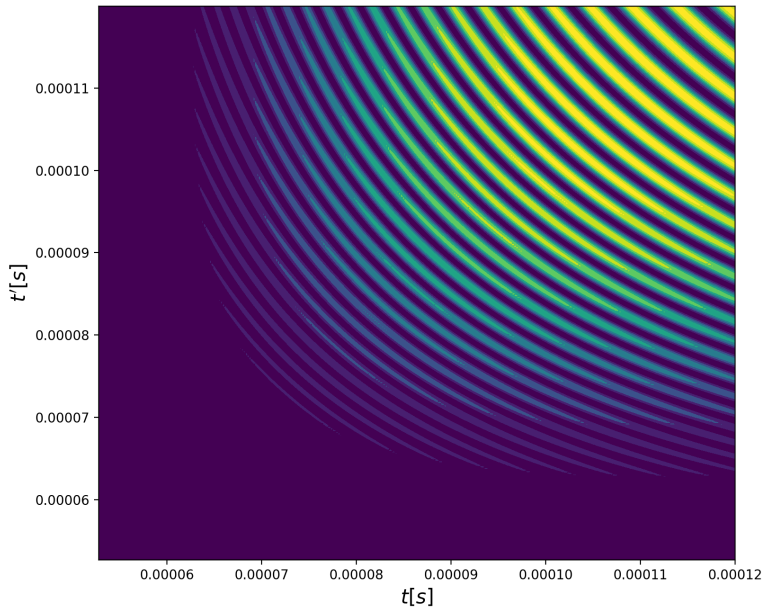

Figure 25: Density plot of $||\Psi_{AB}((x_{DA}, t), (x_{DB}, t'))||^2$ as a function of t and t'.

We see that slicing the interference pattern vertically (fixed time t for particle A), as well as slicing the interference pattern horizontally (fixed time t' for particle B), leads to a conditional interference pattern. However, it should be noted that to produce quantitative results the calculation of $||\Psi_{AB}((x_{DA}, t), (x_{DB}, t'))||^2$ does not suffice. The problem is that implicitly we are still considering perfect position measurements, only that now they are carried out at different times. It turns out that there exist several inequivalent theoretical approaches to calculate the TOA and there is no universally agreed-on solution. For a recent approach and further references see [56].
It should also be mentioned that since we now observe the particles at different times t, t', one has to make sure that the detection events are still space-like separated. For if they are not, factorability can not be assumed anymore.

4 Summary and Outlook

In this thesis the connection between quantum interference and Bell's Theorem was investigated. While in the part A of this thesis, the meaning of quantum interference and Bell's Theorem for the discussion about the interpretation of quantum mechanics was discussed, in the part B of this thesis a two-particle quantum interference thought experiment was developed and the connection between quantum interference and Bell's Theorem was investigated by asking, whether Bell's Theorem can be proven from the available two-particle quantum interference in the considered thought experiment.

By constructing an analogy between measurements on spin-$\frac{1}{2}$ particles in a Stern-Gerlach magnet and the position measurements in the considered thought experiment, it was found that Bell's theorem can be proven in the context of our thought experiment, if certain events in the considered thought experiment are inherently indeterministic.

It remains the question in how far this assumption (that the relevant events are inherently indeterministic) is justified. While there is certainly no empirical evidence against it, it is also difficult (if not impossible) to exclude the possibility of an underlying deterministic origin of these events. In this respect the argumentation in section 2.10, which relied on quantum mechanical complementarity and more specifically the trade-off relation (43), was not able to rule out determinism in principle. However, by showing that in a world, where (43) holds, it is in principle impossible to observe any sign of determinism for certain quantum mechanical phenomena, at least from an empirical point of view a strong argument for the inherent indeterminism of certain quantum mechanical phenomena has been presented.

But even if it is granted that events, for which in principal no sign of determinism can be found, are inherently indeterministic, it is not clear, whether the relevant events in our thought experiment belong to that category. This follows on one hand from the fact, that the trade-off relation (43) has only been tested for a small number of physical systems and that further empirical evidence for the correctness of (43) would be needed and on the other hand from the unproven assumption that the generalization from spin-$\frac{1}{2}$ particles to more general quantum systems in section 2.10 was valid. While we believe that further experimental tests will not find any violation of the quantum mechanical prediction (43) and that at least for the relevant events in our thought experiment the generalization was valid, it is up to further research to close these loopholes.

It should also be mentioned that even though the analysis of this thesis was focussed on a specific experimental configuration, the analogy between spin measurements in an orientable Stern-Gerlach magnet and position measurements in two-particle interference experiments should hold for *all* two-particle interference experiments, which are conceptually similar to the DDS experiment with highly correlated momenta. One could, for example, use the same analogy for the DDS-experiments with photons [2] or electrons [3], which have already been realized experimentally.

Another interesting line of further research in connection to our thought experiment could be to consider the possibility of active choices in terms of applying E-fields with different strengths. Since the main reason for the necessity of invoking indeterminism was the "static character" of our experiment, which did not involve choices of measurement configurations by external agents, this could open new doors for a more traditional proof of Bell's Theorem, where statistical independence is made plausible by a proper spacetime configuration and the free choices of external observers.

5 Appendix

5.1 Conditional Probabilities

This section is meant to clarify our notation for conditional probabilities and to recall some basic properties.

We express the conditional probability that A is true given that B is true by the symbol $P(A|B)$ or sometimes also in the more compressed form $P_B(A)$. Formally, the conditional probability $P(A|B)$ is defined by the equation

$$P(A|B) = \frac{P(A,B)}{P(B)}, \tag{79}$$

where $P(B)$ is the probability, that B is true and $P(A,B)$ is the probability that A *and* B are true. From the definition (79) follows the identity

$$P(A,B|C) = P(A|B,C)P(B|C). \tag{80}$$

If $P(A|B,C) = P(A|B)$ one might say that the condition B *screens off* the condition C with respect to the proposition A, i.e. adding the condition C does not change anything about the probability of A. In this case (80) simplifies to

$$P(A,B|C) = P(A|B)P(B|C). \tag{81}$$

Another important identity, which also follows from the definition (79) is:

$$P(A|B) = \frac{P(B|A)P(A)}{P(B)}. \tag{82}$$

Equation (82) is known as *Bayes' Theorem.*

5.2 Quantitative Complementarity

Considering a spin-$\frac{1}{2}$ system, we show that in quantum mechanics it is impossible to prepare an experiment with outcome probabilities $P(0_x) = P(0_y) = 1/2$, $P(0_z) = 1$ and simultaneously fulfill that $P(0_x|b_j)$ is equal to 0 or 1 for some measurable event b_j, where e.g. $P(0_x)$ is the probability to find spin-up along the x-axis.

In order to show this, we consider a bipartite physical system AB. The result then follows as a direct consequence of the trade-off relation (11), which was:

$$\mathcal{P}_i^2 + \mathcal{V}_i^2 + \mathcal{C}_{AB}^2 = 1, \tag{83}$$

where $\mathcal{C}_{AB}$ is the two qubit concurrence, which as we have mentioned in section 2.3 is an entanglement measure and fulfills $\mathcal{C}_{AB} = 0$, if and only if the state of the system is separable. We recall that for the two qubit state

$$|\Psi_{AB}\rangle = c_1 |0_A\rangle |0_B\rangle + c_2 |0_A\rangle |1_B\rangle + c_3 |1_A\rangle |0_B\rangle + c_4 |1_A\rangle |1_B\rangle \tag{84}$$

the predictabilities $\mathcal{P}_i$, visibilities $\mathcal{V}_i$, and the concurrence $\mathcal{C}_{AB}$ are given by:

$$\begin{aligned} \mathcal{P}_A &= |||c_3||^2 + ||c_4||^2 - ||c_1||^2 - ||c_2||^2| \\ \mathcal{P}_B &= |||c_2||^2 + ||c_4||^2 - ||c_1||^2 - ||c_3||^2| \end{aligned} \tag{85}$$

$$\begin{aligned} \mathcal{V}_A &= 2|c_1 c_3^* + c_2 c_4^*| \\ \mathcal{V}_B &= 2|c_1 c_2^* + c_3 c_4^*| \end{aligned} \tag{86}$$

$$\mathcal{C}_{AB} = 2|c_1 c_4 - c_2 c_3| \tag{87}$$

As one can show by using the above definitions, it holds that $\mathcal{P}_A^2 + \mathcal{V}_A^2 = ||\vec{r}_A||^2$, where $\vec{r}_A$ is the Bloch vector of the A-system, which can be used to parametrize all reduced single qubit density matrices $\boldsymbol{\rho}_A$. Since $\vec{r}_A$ can be written as $\vec{r}_A = 2\vec{P}_A - \vec{1}$ [57], where $\vec{P}_A = (P_A(0_x), P_A(0_y), P_A(0_z))$ and $\vec{1} = (1, 1, 1)$, it follows that

$$\mathcal{P}_A^2 + \mathcal{V}_A^2 = (2P_A(0_x) - 1)^2 + (2P_A(0_y) - 1)^2 + (2P_A(0_z) - 1)^2 \tag{88}$$

and combining equation (88) with equation (83) we can write

$$(2P_A(0_x) - 1)^2 + (2P_A(0_y) - 1)^2 + (2P_A(0_z) - 1)^2 + \mathcal{C}_{AB}^2 = 1. \tag{89}$$

A similar relation holds for the B-system. We will assume $|0_A\rangle$ to be the spin-up state along the z-axis for the system A. The system B we want to treat as an environment, which (in dependence of the coefficients c_1, c_2, c_3, c_4) is coupled with a specific strength to A. We know that the above probabilities $P(0_x) = P(0_y) = 1/2$, $P(0_z) = 1$ are

produced, if the two-particle system is initialized in the separable state

$$|\Psi_{AB}(t_0)\rangle = \exp(i\varphi)\,|0_A\rangle\,|\psi_B\rangle\,, \tag{90}$$

where φ is an arbitrary phase factor and $|\psi_B\rangle$ is an arbitrary state of the environment B. However, in this case quantum mechanics predicts that no event b_j can be found such that $P(0_x|b_j)$ is equal to 0 or 1. We thus ask for a state $|\tilde{\Psi}_{AB}(t_0)\rangle$ such that both conditions are fulfilled and we will show that such a state can not exist.
First we note that no separable state can suffice. For any A-state preparation, which we could identify[24] with b_j such that $P(0_x|b_j)$ is equal to 0 or 1 (one would need to prepare a state of the form $\exp(i\varphi)\,|0_x\rangle$ or $\exp(i\varphi)\,|1_x\rangle$) implies a change of the probabilities $P(0_x) = P(0_y) = 1/2$, $P(0_z) = 1$ and as long as the state is separable no B-measurement result can fulfill the relation $P(0_x|b_j)$ is equal to 0 or 1. We thus have to conclude that $|\tilde{\Psi}_{AB}(t_0)\rangle$ must be entangled. However, entanglement implies that

$$\mathcal{C}^2_{AB} > 0 \tag{91}$$

and $P(0_x) = P(0_y) = 1/2$, $P(0_z) = 1$ implies that

$$(2P_A(0_x) - 1)^2 + (2P_A(0_y) - 1)^2 + (2P_A(0_z) - 1)^2 = 1, \tag{92}$$

which leads to a contradiction with equation (89) and therefore proves our claim.

5.3 The Propagator

In this section we introduce basic properties of the quantum mechanical propagator and derive certain identities, which were used in section 3.2.

We can define the (one-dimensional) propagator $K(y, t_1; x, t_0)$ by the equation

$$\psi(y, t_1) = \int_{-\infty}^{\infty} dx K(y, t_1; x, t_0)\psi(x, t_0). \tag{93}$$

Equation (93) tells us that the value of the wave function at (y, t_1) is the sum over all the values of the wave function $\psi(x, t_0)$ for all x weighted with the factor $K(y, t_1, x, t_0)$. One way to think of equation (93) is in terms of Huygen's principle for matter waves

[24] In this case b_j is understood as the observable "preparation-event" of the quantum system, e.g. the configuration of the electron source, which implies a certain spin-orientation etc.

[58]. We can find an explicit expression for the propagator as follows: By resolving the wave function $\psi(x, t_0)$ into a superposition of energy eigenstates, we find that

$$\psi(x, t_0) = \sum_{n,l} \alpha(n, l)\varphi_{nl}(x), \tag{94}$$

where $\varphi_{nl}(x)$ are energy-eigenstates with the energy E_n and the prefactors $\alpha(n, l)$ are complex-valued coefficients. As the energy might be degenerate, another parameter l distinguishes the eigenfunctions with the same energy. The time evolved state $\psi(y, t_1)$ can be expressed as

$$\psi(y, t_1) = \sum_{n,l} \alpha(n, l) \exp\Big(- \frac{i}{\hbar} E_n(t_1 - t_0)\Big)\varphi_{nl}(y). \tag{95}$$

We further know that by definition

$$\alpha(n, l) = \int_{-\infty}^{\infty} dx \varphi^*_{nl}(x)\psi(x, t_0) \tag{96}$$

and substituting equation (96) into equation (95) leads to:

$$\psi(x, t_1) = \int_{-\infty}^{\infty} dx \sum_{n,l} \varphi_{nl}(y)\varphi^*_{nl}(x) \exp\Big(- \frac{i}{\hbar} E_n(t_1 - t_0)\Big)\psi(x, t_0). \tag{97}$$

Comparison with (93) gives the following expression for the propagator in terms of energy eigenfunctions:

$$K(y, t_1; x, t_0) = \sum_{n,l} \varphi_{nl}(y)\varphi^*_{nl}(x) \exp\Big(- \frac{i}{\hbar} E_n(t_1 - t_0)\Big). \tag{98}$$

Another way to express the quantum mechanical propagator is given by Feynman's path integral formalism [58]. Symbolically, one can write:

$$K(y, t_1; x, t_0) = \mathcal{N} \int \mathcal{D}x \exp\Big(\frac{i}{\hbar} S_\gamma[y, t_1; x, t_0]\Big). \tag{99}$$

According to Feynman, the propagator can be understood as a sum over paths, where each path γ contributes a summand of the form $N_\gamma \exp(\frac{i}{\hbar} S_\gamma[y, t_1; x, t_0])$. Here, N_γ is a normalization constant and $S_\gamma[y, t_1; x, t_0]$ is the action along the path γ with end-points

y and x. It holds accordingly that

$$K(y,t_1;x,t_0) = \sum_\gamma N_\gamma \exp(\frac{i}{\hbar} S_\gamma[y,t_1;x,t_0]). \tag{100}$$

By considering time-steps t_i, which are separated from each other by the small interval ϵ, and then taking the limit $\epsilon \to 0$, it can be shown that[25] equation (100) can be rewritten as

$$K(y,t_1;x,t_0) = \lim_{\epsilon\to 0}\Big(\frac{2\pi i\hbar\epsilon}{m}\Big)^{\frac{N}{2}} \int\int\int ... \exp\Big(\frac{i}{\hbar} S[y,t_1;x,t_0]\Big) dx_1 dx_2 ... dx_{N-1}. \tag{101}$$

Equation (101) is equivalent to the symbolical expression (99). The proof that expression (101) fulfills (93) is for example given in [58].

5.3.1 Free Particle

For the free particle the energy eigenfunctions are given by:

$$\varphi_p(x) = \exp\Big(-\frac{i}{\hbar} px\Big). \tag{102}$$

Plugging these relations into (98) the free particle propagator turns out to be:

$$K_F(y,t_1;x,t_0) = \int_{-\infty}^{\infty} dp \exp\Big(\frac{i}{\hbar} p(y-x)\Big) \exp\Big(\frac{i}{\hbar}\frac{p^2}{2m}\Delta t\Big). \tag{103}$$

The integrand in (103) is a gaussian function with respect to momentum p and the integration can be carried out directly, which leads to

$$K_F(y,t_1;x,t_0) = \sqrt{\frac{m}{2\pi\hbar i\Delta t}} \exp\Big(\frac{im}{2\hbar}\frac{(y-x)^2}{\Delta t}\Big). \tag{104}$$

We could have equally well evaluated the path integral

$$K_F(y,t_1;x,t_0) = \mathcal{N}\int \mathcal{D}x \exp\Big(\int_{t_0}^{t_N} dt \frac{1}{2} m\dot{x}^2\Big), \tag{105}$$

[25] We have set $t_1 = t_N$ and $y = x_N$, $x = x_0$. Equation (101) is only true if the lagrangian is of the form:

$$L = \frac{1}{2} m\dot{x}^2 - V(x)$$

which, however, covers all the relevant cases.

which would have given the same result (104).

5.3.2 Particle in a Constant Electric Field

There exist several equivalent approaches to derive the propagator for the particle in a constant electric field [59, 60]. We will consider Feynman's path integral method. The one dimensional Lagrangian for a constant force $F = qE$, where q is the charge of the particle and E is the electric field strength of the electric field is given by:

$$L = T - V = \frac{1}{2}m\dot{x}^2 + Fx. \tag{106}$$

We want to consider this Lagrangian for all paths from a specified starting point x_0 to a specified endpoint x_N. We can parametrize these paths by thinking of all paths as deviations y from the classical path x_{cl}. With this conception we can rewrite the lagrangian as

$$L = \frac{1}{2}m(\dot{x}_{cl} + \dot{y})^2 + F(x_{cl} + y) = \Big(\frac{1}{2}m\dot{x}_{cl}^2 + Fx_{cl}\Big) + \Big(m\dot{x}_{cl}\dot{y} + Fy\Big) + \frac{1}{2}m\dot{y}^2. \tag{107}$$

The time integral over the second term on the right hand side of (107) is zero, as can be seen by partial integration:

$$\int_{t_0}^{t_N} dt\Big(m\dot{x}_{cl}\dot{y} + Fy\Big) = m\dot{x}_{cl}y\Big|_{t_0}^{t_N} - \int_{t_0}^{t_N} dtm\ddot{x}_{cl}y + \int_{t_0}^{t_N} dtFy = 0, \tag{108}$$

where the last equality follows from $m\ddot{x}_{cl} = F$ and the vanishing deviation ($y = 0$) at t_0 and t_N. The remaining path integral is

$$K_E(y, t_1; x, t_0) = \exp\Big(\int_{t_0}^{t_N} dt\Big(\frac{1}{2}m\dot{x}_{cl}^2 + Fx_{cl}\Big)\Big)\mathcal{N}\int \mathcal{D}y \exp\Big(\int_{t_0}^{t_N} dt\frac{1}{2}m\dot{y}^2\Big). \tag{109}$$

From equation (105) we know that this can be rewritten as

$$K_E(y, t_1; x, t_0) = \exp\Big(\int_{t_0}^{t_N} dt\Big(\frac{1}{2}m\dot{x}_{cl}^2 + Fx_{cl}\Big)\Big)\sqrt{\frac{m}{2\pi\hbar i\Delta t}}\exp\Big(\frac{im}{2\hbar}\frac{(y-x)^2}{\Delta t}\Big). \tag{110}$$

To evaluate the remaining integral, we consider the classical trajectory

$$x_{cl}(t) = x_0 + v_0(t - t_0) + \frac{1}{2}\frac{F}{m}(t - t_0)^2. \tag{111}$$

If we set

$$t_0 = 0; \qquad x_{cl}(t_N) := x_N, \tag{112}$$

we obtain

$$\int_{t_0}^{t_N} dt\Big(\frac{1}{2}m\dot{x}_{cl}^2 + Fx_{cl}\Big) = \frac{m}{2}\frac{(x_N - x_0)^2}{t_N - t_0} + \frac{1}{2}F(t_N - t_0)(x_N + x_0) - \frac{1}{24}\frac{F^2}{m}(t_N - t_0)^3. \tag{113}$$

Combining equation (113) with (110) leads to the final result:

$$K_E(y, t_1; x, t_0) = \sqrt{\frac{m}{2\pi\hbar i\Delta t}}\exp\Big(\frac{i}{\hbar}\Big\{\frac{m(y-x)^2}{2\Delta t} + \frac{F\Delta t(y+x)}{2} - \frac{1}{24}F^2\Delta t^3\Big\}\Big). \tag{114}$$

5.3.3 Fourier-Transform Representation

We can represent the integral transform

$$\psi(y, t_1) = \int_{-\infty}^{\infty} dx K(y, t_1; x, t_0)\psi(x, t_0) \tag{115}$$

for the propagators $K_F(y, t_1; x, t_0)$ and $K_E(y, t_1; x, t_0)$ in terms of a Fourier-transform ($\mathcal{F}$) and a subsequent backtransform ($\mathcal{F}^{-1}$). For the free particle propagator this is already implied by equation (103), which we can simply rewrite as

$$\psi(y, t) = \mathcal{F}^{-1}\Big\{\exp\Big(-i\hbar\frac{k^2}{2m}\Delta t\Big)\mathcal{F}(\psi(x, t_0))\Big\}. \tag{116}$$

For the constant E-field propagator we consider the expression

$$K_E(y, t_1; x, t_0) = C_1\int_{-\infty}^{\infty} dk\exp\Big(i\Big[k(y-x) + C(y, x, \Delta t)\Delta t - \frac{\hbar k^2}{2m}\Delta t - \frac{F}{m}k\Delta t^2\Big]\Big) \tag{117}$$

with

$$\begin{aligned} C_1 &= \frac{1}{2\pi}, \\ C(y, x, \Delta t) &= \frac{1}{\hbar}\Big\{\frac{3}{2}yF - \frac{13}{24m}F^2\Delta t^2 - \frac{1}{2}xF\Big\}. \end{aligned} \tag{118}$$

By the use of (117) we can write the integral transform (115) for $K_E(y, t_1, x, t_0)$ as

$$\psi(y,t) = g(\Delta t)\mathcal{F}^{-1}\Big\{ \exp\Big(- i\Big[\frac{F}{m}k\Delta t^2 + \hbar\frac{k^2}{2m}\Delta t\Big]\Big)\mathcal{F}\Big\{ \exp\Big(- \frac{i}{2\hbar}xF\Delta t\Big)\psi(x,t_0)\Big\}\Big\}; \tag{119}$$

$$g(\Delta t) = \exp\Big(\frac{i}{\hbar}\Big[\frac{3}{2}yF\Delta t - \frac{13}{24m}F^2\Delta t^3\Big]\Big). \tag{120}$$

6 References

[1] D.M. Greenberger, M. A. Horne, and A. Zeilinger. Multiparticle Interferometry and the Superposition Principle. *Physics Today*, 1993.

[2] M. Kaur and M. Singh. Quantum double-double-slit experiment with momentum entangled photons. *Scientific Reports*, 2020.

[3] M. Waitz, D. Metz, J. Lower, C. Schober, M. Keiling, M. Pitzer, K. Mertens, M. Martins, J. Viefhaus, S. Klumpp, T. Weber, H. Schmidt-Böcking, L. Ph H. Schmidt, F. Morales, S. Miyabe, T. N. Rescigno, C. W. McCurdy, F. Martín, J. B. Williams, M. S. Schöffler, T. Jahnke, and R. Dörner. Two-Particle Interference of Electron Pairs on a Molecular Level. *Physical Review Letters*, 2016.

[4] J. Kofler, M. Singh, M. Ebner, M. Keller, M. Kotyrba, and A. Zeilinger. Einstein-Podolsky-Rosen correlations from colliding Bose-Einstein condensates. *Physical Review A - Atomic, Molecular, and Optical Physics*, 2012.

[5] C. Gneiting and K. Hornberger. Nonlocal Young tests with Einstein-Podolsky-Rosen-correlated particle pairs. *Physical Review A - Atomic, Molecular, and Optical Physics*, 2013.

[6] M. C. Tichy, F. Mintert, and A. Buchleitner. Essential entanglement for atomic and molecular physics, 2011.

[7] J. S. Bell. On the Einstein Podolsky Rosen paradox. *Physics 1*, 1964.

[8] N. David Mermin. Is the moon there when nobody looks? reality and the quantum theory. *Physics Today*, 38(4):38–47, 1985.

[9] C. Jönsson. Elektroneninterferenzen an mehreren künstlich hergestellten Feinspalten. *Zeitschrift für Physik*, 1961.

[10] A. Zeilinger, R. Gähler, C. G. Shull, W. Treimer, and W. Mampe. Single- and double-slit diffraction of neutrons. *Reviews of Modern Physics*, 1988.

[11] M. Arndt, O. Nairz, J. Vos Andreae, C. Keller, G. Van der Zouw, and A. Zeilinger. Wave–particle duality of C/sub 60/ molecules. *Nature*, 1999.

[12] J. Wolfe. Diffraction from a single slit. Young's experiment with finite slits. https://www.animations.physics.unsw.edu.au/jw/light/single-slit-diffraction.html.

[13] R. P. Feynman and A. R. Hibbs. The Fundamental Concepts of Quantum Mechanics. In *Quantum Mechanics and Path Integrals*, chapter 1. Dover Books on Physics, emended edition, 2010.

[14] D. Bohm. A suggested interpretation of the quantum theory in terms of "hidden" variables. I. *Physical Review*, 1952.

[15] D. Bohm. A suggested interpretation of the quantum theory in terms of "hidden" variables. II. *Physical Review*, 1952.

[16] M. Gondran and A. Gondran. Numerical simulation of the double slit interference with ultracold atoms. *American Journal of Physics*, 2005.

[17] N. Bohr. Diskussionen mit Einstein über erkenntnistheoretische Probleme in der Atomphysik. In *Atomphysik und menschliche Erkenntnis*, chapter 4. Vieweg und Sohn, 1985.

[18] D. Bohm. Wave vs. Particle Properties of Matter. In *Quantum Theory*, chapter 6. Dover Books on Physics, 1989.

[19] W. K. Wootters and W. H. Zurek. Complementarity in the double-slit experiment: Quantum nonseparability and a quantitative statement of Bohr's principle. *Physical Review D*, 1979.

[20] D.M. Greenberger and A. Yasin. Simultaneous wave and particle knowledge in a neutron interferometer. *Physics Letters A*, 1988.

[21] B. Falkenburg. Wave-Particle Duality. In *Particle Metaphysics: A Critical Account of Subatomic Reality*, chapter 7. Springer-Verlag, 2007.

[22] M. Masi. Advanced experimental tests of "quantum ontology". In *Quantum Physics: An Overview of a Weird World Volume II*, chapter 1. Second edition, 2020.

[23] M. Jakob and J. A. Bergou. Quantitative complementarity relations in bipartite systems: Entanglement as a physical reality. *Optics Communications*, 2010.

[24] S. Hill and W. K. Wootters. Entanglement of a Pair of Quantum Bits. *Physical Review Letters*, 1997.

[25] W. K. Wootters. Entanglement of formation of an arbitrary state of two qubits. *Physical Review Letters*, 1998.

[26] W. Heisenberg. Über den anschaulichen Inhalt der quantentheoretischen Kinematik und Mechanik. *Zeitschrift für Physik*, 1927.

[27] Anton Zeilinger. A foundational principle for quantum mechanics. *Foundations of Physics*, 1999.

[28] D. Bohm. Quantum Theory and the Process of Measurement. In *Quantum Theory*, chapter 22. Dover Books on Physics, 1989.

[29] J. Von Neumann. *Mathematische Grundlagen der Quantenmechanik*. Springer-Verlag, 1996.

[30] H. Everett. *The Theory of the Universal Wave Function*. PhD thesis, Princeton, 1656.

[31] J. A. Barrett. *The Quantum Mechanics of Minds and Worlds*. Oxford University Press, 2012.

[32] J.A. Barrett. Many Histories. In *The Quantum Mechanics of Minds and Worlds*, chapter 8. Oxford University Press, 2001.

[33] Y. Aharonov and D. Z. Albert. Can we make sense out of the measurement process in relativistic quantum mechanics? *Physical Review D*, 1981.

[34] J. A. Barrett. The Standard Formulation of Quantum Mechanics. In *The Quantum Mechanics of Minds and Worlds*. Oxford University Press, 2001.

[35] A. Einstein, B. Podolsky, and N. Rosen. Can quantum-mechanical description of physical reality be considered complete? *Physical Review*, 1935.

[36] N. Bohr. Can quantum-mechanical description of physical reality be considered complete? *Physical Review*, 1935.

[37] A. G. Valdenebro. Assumptions underlying Bell's inequalities. *European Journal of Physics*, 2002.

[38] A. Aspect, P. Grangier, and G. Roger. Experimental tests of realistic local theories via Bell's theorem. *Physical Review Letters*, 1981.

[39] A. Aspect, P. Grangier, and G. Roger. Experimental realization of Einstein-Podolsky-Rosen-Bohm Gedankenexperiment: A new violation of Bell's inequalities. *Physical Review Letters*, 1982.

[40] A. Aspect, J. Dalibard, and G. Roger. Experimental test of Bell's inequalities using time- varying analyzers. *Physical Review Letters*, 1982.

[41] B. Hensen, H. Bernien, A. E. Dreaú, A. Reiserer, N. Kalb, M. S. Blok, J. Ruitenberg, R. F.L. Vermeulen, R. N. Schouten, C. Abellán, W. Amaya, V. Pruneri, M. W. Mitchell, M. Markham, D. J. Twitchen, D. Elkouss, S. Wehner, T. H. Taminiau, and R. Hanson. Loophole-free Bell inequality violation using electron spins separated by 1.3 kilometres. *Nature*, 2015.

[42] M. Giustina, M. A.M. Versteegh, S. Wengerowsky, J. Handsteiner, A. Hochrainer, K. Phelan, F. Steinlechner, J. Kofler, J. Å. Larsson, C. Abellán, W. Amaya, V. Pruneri, M. W. Mitchell, J. Beyer, T. Gerrits, A. E. Lita, L. K. Shalm, S. W. Nam, T. Scheidl, R. Ursin, B. Wittmann, and A. Zeilinger. Significant-Loophole-Free Test of Bell's Theorem with Entangled Photons. *Physical Review Letters*, 2015.

[43] L. K. Shalm, E. Meyer-Scott, B. G. Christensen, P. Bierhorst, M.A. Wayne, M. J. Stevens, T. Gerrits, S. Glancy, D. R. Hamel, M. S. Allman, K. J. Coakley, S. D. Dyer, C. Hodge, A. E. Lita, V. B. Verma, C. Lambrocco, E. Tortorici, A. L. Migdall, Y. Zhang, D. R. Kumor, W. H. Farr, F. Marsili, M. D. Shaw, J. A. Stern, C. Abellán, W. Amaya, V. Pruneri, T. Jennewein, M. W. Mitchell, P.G. Kwiat, J. C. Bienfang, R.P. Mirin, E. Knill, and S. W. Nam. Strong Loophole-Free Test of Local Realism. *Physical Review Letters*, 2015.

[44] D. Z. Albert. Bohm's Theory. In *Quantum Mechanics and Experience*, chapter 7. Harvard University Press, 1992.

[45] J.A. Barrett. Selecting a Branch. In *The Quantum Mechanics of Minds and Worlds*, chapter 5. Oxford University Press, 2001.

[46] S. Hossenfelder and T. Palmer. Rethinking Superdeterminism. *Frontiers in Physics*, 2020.

[47] K. Landsman. Indeterminism and Undecidability. 2021.

[48] X. F. Qian, K. Konthasinghe, S. K. Manikandan, D. Spiecker, A. N. Vamivakas, and J. H. Eberly. Turning off quantum duality. *Physical Review Research*, 2020.

[49] V. Jacques, E. Wu, F. Grosshans, F. Treussart, P. Grangier, A. Aspect, and J. Roch. Delayed-choice test of quantum complementarity with interfering single photons. *Physical Review Letters*, 2008.

[50] S. Dürr, T. Nonn, and G. Rempe. Fringe visibility and which-way information in an atom interferometer. *Physical Review Letters*, 1998.

[51] D. G. Arbó, C. Lemell, S. Nagele, N. Camus, L. Fechner, A. Krupp, T. Pfeifer, S. D. López, R. Moshammer, and J. Burgdörfer. Ionization of argon by two-color laser pulses with coherent phase control. *Physical Review A - Atomic, Molecular, and Optical Physics*, 2015.

[52] M. Ferray, A. L'Huillier, X. F. Li, L. A. Lompre, G. Mainfray, and C. Manus. Multiple-harmonic conversion of 1064 nm radiation in rare gases. *Journal of Physics B: Atomic, Molecular and Optical Physics*, 1988.

[53] E. L. Falcão-Filho, C. J. Lai, K. H. Hong, V. M. Gkortsas, S. W. Huang, L. J. Chen, and F. X. Kärtner. Scaling of high-order harmonic efficiencies with visible wavelength drivers: A route to efficient extreme ultraviolet sources. *Applied Physics Letters*, 2010.

[54] R. P. Feynman and A. R. Hibbs. Measurements and Operators. In *Quantum Mechanics and Path Integrals*, chapter 5. Dover Books on Physics, emended edition, 2010.

[55] J. Ullrich, R. Moshammer, A. Dorn, R. Dörner, L. Ph H. Schmidt, and H. Schmidt-Böcking. Recoil-ion and electron momentum spectroscopy: Reaction-microscopes. *Reports on Progress in Physics*, 2003.

[56] D. Jurman and H. Nikolić. The time distribution of quantum events. *Physics Letters, Section A: General, Atomic and Solid State Physics*, 2021.

[57] Philipp Andres Höhn. Toolbox for reconstructing quantum theory from rules on information acquisition. *Quantum*, 2017.

[58] R. P. Feynman. Space-Time Approach to Non-Relativistic Quantum Mechanics, 1948.

[59] F. Soto-Eguibar and H. M. Moya-Cessa. Solution of the Schrodinger Equation for a Linear Potential using the Extended Baker-Campbell-Hausdorff Formula. *Applied Mathematics and Information Sciences*, 2015.

[60] N. Wheeler. Classical/Quantum Dynamics in a Uniform Gravitational Field: A. Unobstructed Free Fall, 2002.

Erklärung:

Ich versichere, dass ich diese Arbeit selbstständig verfasst habe und keine anderen als die angegebenen Quellen und Hilfsmittel benutzt habe.

Berlin, den 28. Oktober 2021 .....